

Acknowledgments

We would like to thank our tutor S.Jesus for accompanying us all the way throughout this Final Year Project with his expertise and warm welcome at the University of Algarve (UALG). We also thank him for trying hard to make us take part in the Azores' experiment and for providing us with substitution data.

We sincerely thank Professor Guillon, in charge of the Underwater Acoustics class, for giving us advice regarding substitution experiments and for contacting Major Dreo, to whom we are grateful for his acoustic identification of the samples we had sent him.

We are grateful to our pilot officer Lieutenant commander Varigny and our English teacher Ms. Simoneau-Byrne for their rereading work and the tips given to produce this report.

Lastly, we would like to truly thank all the professors and the administrative staff of the French Naval Academy for enabling us to pursue this Final Year Project.

Abstract

Students : EV2 Victor DAUMAS, EV2 Audrain PROUCHET, E.N. 17
Major : Underwater Acoustics
Host organization : SiPLAB, University of Algarve (UALG)
Project tutor : Sérgio M. Jesus
Jury chairman : Jean-Marc le Caillec

Résumé

La notion de localisation en acoustique sous-marine est parfois associée à la surveillance acoustique passive et fait aujourd'hui l'objet de différents enjeux scientifiques et militaires: localiser sans être détecté. Différents systèmes et méthodes ont vu le jour pour localiser une source sonore: bouées sonores, assemblage d'hydrophones remorqués ou fixes, etc. Dans le cadre du projet JONAS, un AUV de type wave glider a été développé pour effectuer une traversée entre les Açores et les Canaries. La contrainte qui nous a été donnée était d'y fixer quatre hydrophones pour détecter et localiser les signaux de cétacés enregistrés. A cet égard, nous avons étudié et simulé deux méthodes de localisation de cétacés. Ensuite, nous avons appliqué les programmes développés à de la donnée expérimentale qui ne correspondait pas tout à fait à l'expérience du projet JONAS initialement prévue. Enfin, ce projet a pu mettre en lumière la détection de différents types de signaux émis par des mammifères marins ainsi que deux méthodes de localisation différentes: une estimation de la direction d'arrivée des signaux et une estimation de la profondeur de la source.

Abstract

The notion of localization in underwater acoustic is sometimes associated to passive acoustic monitoring and is nowadays the topic of various scientific and military stakes: localize without being detected. Different methods have emerged in order to localize a sound source: sonobuoys, towed or fixed hydrophones arrays, etc. In the frame of the JONAS project, an AUV, namely a wave glider, on which hydrophones can be fixed was developed to travel from the Azores to the Canaries. The constraint we were given was to fix four hydrophones to the AUV in order to detect and localize the recorded cetacean signals. In this regard, we have studied and simulated two localization methods. Then, we applied the developed programs to experimental data that did not quite correspond to the JONAS experiment initially planned. Finally, this project enabled us to highlight the detection of different types of signals emitted by marine mammals as well as two different localization methods: direction-finding estimation and depth estimation.

Keys words: PAM, localization, cetacean, cross-correlation, signals

Presentation

SiPLAB is a laboratory located in the University of Algarve (UALG), and more precisely in the faculty of Sciences and Technologies, gathering university professors, researchers and students studying signal processing, underwater acoustics and communications. SiPLAB is part of the Signal Processing Group (SIPg) of ISR - Instituto de Sistemas e Robótica and itself member of the Associated Laboratory LARSys. SiPLAB's main sponsor for projects is CINTAL.

We were first proposed to study the stake of cetacean localization with a AUV with four fixed hydrophones in regard of the JONAS project: Joint framework for Ocean Noise in the Atlantic Seas. Even though the project was not directed towards cetacean localization issues, the collected data was meant to enable cetacean signal detection. JONAS studies the threats to biodiversity from underwater noise pollution on sensitive species in the NE Atlantic by streamlining ocean noise monitoring and risk management on a transnational basis. JONAS developed a autonomous noise-monitoring platform, namely a wave glider, that will travel from the Azores to the Canary islands.

We finally worked on data recorded in the frame of the SUB-ECO project. Funded by the Ministry of Defense (Portugal), this project aims at reinforcing the capabilities of national underwater surveillance using passive detection of illicit activities of both surface and submerged ships off the coast of Portugal. The data of this project that we used to localize cetaceans was first recorded with a tetrahedron six-hydrophone array hung under a buoy as a trial phase.



UALg

UNIVERSIDADE DO ALGARVE

SiPLABoratory

Contents

List of figures	5
List of tables	6
Abbreviations	7
Glossary	8
Introduction	9
I- Passive Acoustic Monitoring (PAM) of cetaceans: basics, environment and cetacean sound sources	10
A- Underwater acoustics: the basics	10
1- Principle of underwater acoustics	10
2- Cetacean sounds	11
B - The environment and the means of interest of the experiment	11
1 - The Azores' and Lisbon's environment	12
2 - The means: AUVs	15
C - Simulation of the target	16
1 - The sound source: the beaked whale	17
2 - Numeric simulation of the sound source: beaked whale clicks	18
II - Methods of localization for a four-hydrophone planar array	21
A - Signal detection methods and time of arrival measurement	21
1 - Detection	21
2 - Measurement of time difference of arrival: cross-correlation	21
B - First method of localization: bearing estimation (direction finding)	23
1 - Azimuth and elevation finding method	23
2 - Simulation of the method	25
C - Second method of localization: depth estimation	28
1 - Depth localization principle	28
2 - Numerical simulation	29
III - Application of localization methods to an experimental four-hydrophone array	33
A - The localization experiment	33
1 - The experiment	33
2 - The exploitation of the data	34
3 - Time Difference Of Arrival measurement	37
B - Results and analysis	40
1 - Bearing estimation	40
2 - Depth estimation	42
Conclusion	45
Appendix A - Matlab functions	46
Appendix B - Table results	48
Bibliography	49

List of figures

Figure 1 - Mapping of the Azores (left panel) and of the area of interest (right panel)	12
Figure 2 - Mapping off Lisbon's coast (upper panel) and of the area of interest (lower panel).....	13
Figure 3 - SSP and ray paths of the Azores compared to a constant SSP	14
Figure 4 - SSP and ray paths off Lisbon's coast compared to a constant SSP	14
Figure 5 - Example of a slocum glider diving profile	15
Figure 6 - Wave glider (left panel) and the overall dimensions and attachment points (left panel)	16
Figure 7 - Time domain beaked whale clicks	17
Figure 8 - Examples of waveform (upper panels) and spectrograms (lower panels) of different beaked whales	18
Figure 9 - Cuvier's beaked whale clicks' waveform (upper panel) and spectrogram (lower panel) extracted from the 2013 towed hydrophone array data	19
Figure 10 - Waveform and spectrogram of three simulated clicks.....	19
Figure 11 - Simulation of the waveform (upper panels) and spectrogram (lower panels) of one emitted click signal (left panels) and of the received signal by an hydrophone (right panels).....	20
Figure 12 - MATLAB cross-correlation simulation with two delayed noisy Ricker signals	22
Figure 13 - Estimation of sound arrival angle	23
Figure 14 - Angles for two-dimensional constrained direction-finding	24
Figure 15 - Calculated azimuth (left panel) and elevation (right) for a fixed distance and azimuth in function of the elevation angle	27
Figure 16 - Time difference of arrival for a fixed distance and elevation in function of the azimuth angle before (left panel) and after (right panel) filtering the received signal	23
Figure 17 - Calculated azimuth (left panel) and elevation (right) for a fixed distance and azimuth in function of the elevation angle	23
Figure 18 - Calculated azimuth (left panel) and elevation (right) for a fixed distance and elevation in function of the azimuth angle.....	23
Figure 19 - Geometry and elevation angle ϑ	23
Figure 20 - Calculated and theoretical depth for a fixed distance and azimuth in function of the elevation angle.....	323

Figure 21 - Estimated depth depending on the estimated elevation error	33
Figure 22 - Representation of the diamond hydrophone array	35
Figure 23 - Comparison of two spectrums of the audio file 0056 before (left panel) and after (right panel) filtering.....	36
Figure 24 - Spectrums of files 0048 (left panel) containing frequency peak around 5 kHz and 12 kHz and 0099 (right panel) with a concentration of acoustic energy above 20 kHz.....	37
Figure 25 – Spectrogram of cetacean whistles	37
Figure 26 – Spectrogram of cetacean clicks	38
Figure 27 - Spectrogram of cetacean whistles and clicks (source: intern data 057.wav)	39
Figure 28 - Waveform of cetacean whistles and clicks (source: intern data 057.wav)	40
Figure 29 - Spectrogram of cetacean clicks, audio file 092.wav	40
Figure 30 - Waveform of cetacean clicks, audio file 092.wav	41
Figure 31 – Waveform of isolated cetacean clicks on channels 1 and 2 (092.wav).....	41
Figure 32 - Spectrogram of isolated cetacean clicks of channel 2 (092.wav)	423
Figure 33 - Estimation azimuth γ and elevation angle ϑ with clicks from three different audio files	44

List of tables

Table 1 - Azimuth and Elevation angles calculated the audio file 0094.wav between 5.51 and 6.15s	41
Table 2 - Calculated depths of file 131.wav for the positive values of the elevation angle	43
Table 3 - Calculated depths of file 131.wav for the negative values of the elevation angle	43

Abbreviations

AUV	:	Autonomous Underwater Vehicle
GEBCO	:	General Bathymetric Charts of the Oceans
GPS	:	Global Positioning System
ICI	:	Inter Click Intervall
JONAS	:	Joint framework for Ocean Noise in the Atlantic Seas
NOAA	:	National Oceanic and Atmospheric Administration
PAM	:	Passive Acoustic Monitoring
SONAR	:	SOund Navigation And Ranging
SNR	:	Sound to Noise Ratio
SSP	:	Sound Speed Profile
TDOA	:	Time Difference Of Arrival
UALG	:	University of ALGarve

Glossary

r	:	range of the sound source	[m]
P	:	pressure of the sound wave	[Pa]
S	:	salinity	[psu]
ICI	:	inter click intervall	[s]
T	:	temperature of the water	[°C]
c	:	celerity of sound	[$m \cdot s^{-1}$]
λ	:	wavelength of a signal	[m]
f	:	frequency of a signal	[Hz]
L	:	distance between hydrophones	[m]
$\delta\tau_{ij}$:	time difference of arrival between two hydrophones H_i and H_j	[s]
h	:	depth of hydrophone	[m]
d	:	depth of the sound source	[m]
β	:	direction of the sound source	[°]
γ	:	azimuth of the sound source	[°]
ϑ	:	elevation of the sound source	[°]

Introduction

Whether it is for scientific or military purposes, the knowledge of underwater animals' or objects' presence has different ecological and operational stakes. The study of this presence, throughout detection, classification or localization, passes through the knowledge of underwater acoustics propagation. Mastering the theory of underwater acoustics makes it possible to implement underwater detection equipment: whether to determine a quantity of cetaceans with hydrophones or detect a submarine with a SONAR. In order to study the movement of these underwater mammals or objects without being detected or harming the cetacean, one may require the use of PAM: Passive Acoustic Monitoring. In this regard, PAM may be broken down as such: detection, classification, localisation and eventually tracking (even though tracking is a direct consequence of localization, as localization on the long term). Within the framework of our Final Year Project, we will focus on the localization part of the process. Moreover, we will study exclusively cetaceans, that is to say sea mammals using echolocation signals to locate oneself. Thereby, the detection and classification processes will be mentioned but not fully developed.

After nearly 70 years of signal processing, many equipment, methods and algorithms have been developed for PAM purposes. In fact, localization of underwater mammals or objects is carried out thanks to the sound made by the source. Depending on the type of seabed and the oceans' characteristics, localization may be performed with varying equipment and methods: hydrophones widely spaced for triangulation, sonobuoys, towed linear arrays and volumetric arrays of hydrophones, bottom mounted systems... Furthermore, scientists are currently studying the possibility of fixing arrays to AUVs (Autonomous Underwater Vehicles) in order to explore different type of seas and deeper environments. In this sense, we have been working on the question of fixing four hydrophones to a wave glider for localization issues in the frame of the JONAS project, which Algarve University (UALG) was contributing to. The aim of this project is to send a wave glider for a two-month trip from the archipelago of the Azores to the Canaries. Initially, a one to two days trial phase was planned just before sending the wave glider during the week of October 21st to test the recording of the hydrophones and assess the AUV's self-noise in the waters of the Azores. In this regard, we had a specification and been working on dimensioning a four-hydrophone array for this trial phase experiment. However, a week before this trial experiment, the wave gliders' shipment was postponed and the trial phase cancelled. Our tutor therefore provided us with substitution data from another recent experiment off Cabo Espichel (Lisbon's' coast) of a six-hydrophone tetrahedron array hung under a buoy in the frame of the SUB-ECO project. Thereby, we decided to keep a part of our previous work and adapt it to the new data by considering only four hydrophones out of the initial array.

The issue of this Final Year Project is to localize cetaceans with a four-hydrophone array fixed to an AUV. In this matter, we may first study passive acoustic monitoring of cetaceans, that is to say, the environment, the signals of interest and the means. Then, the question of localization and two different methods will be considered. Eventually, these localization methods will be extended to Lisbon's experimental data and discussed. Each method will be numerically simulated and each simulation will be analysed and discussed.

I- Passive Acoustic Monitoring (PAM) of cetaceans: basics, environment and cetacean sound sources

Passive acoustic monitoring is an important notion in the scientific field given that it provides a monitoring of sea mammals just by listening to underwater signals. The notion of passiveness prevents the altering of cetacean behaviour and precludes interacting with these mammals. This part enhances the basics of underwater acoustics and PAM, how it works and how it is operated.

A- Underwater acoustics: the basics

Even though “acoustics” recalls the field of audible frequencies and sound propagation in the air, we will here study the phenomena of underwater sound propagation and frequencies other than those audible by the human ear. This part provides general knowledge about underwater acoustics and the sounds emitted by the mammals inhabiting the seas and oceans.

1- Principle of underwater acoustics

In acoustics, as for underwater acoustics, sound describes all pressure waves generated by an initial pressure fluctuation. Sound is then related to the sound wave propagation that emanates from Newton’s second law: sound is therefore directly related to a variation of pressure P . This part presents very roughly the basics of acoustics that will be needed for the rest of the document without going into the details of the equations below.

The solution to the spherical wave equation (1.1) is given by (1.2) which includes outgoing (minus sign) and incoming waves (plus sign).

$$\frac{d^2(rP)}{dt^2} = c^2 \frac{d^2(rP)}{dr^2} \quad (1.1) \quad r \text{ is the range and } t \text{ the time}$$

$$P = \frac{1}{r} f(ct \pm r) \quad (1.2) \quad f \text{ is an independent function}$$

A more appropriate solution to describe waves is the periodic solution. By introducing a cosine periodic function, the function f becomes (1.3).

$$f(r - ct) = A(ct - r). \cos\left(\frac{2\pi}{\lambda}(ct - r)\right) \quad (1.3) \quad \lambda \text{ is the periodicity and } A(ct - r) \text{ the amplitude of the pressure wave, function of } ct-r$$

In the simplest case, sound propagates at constant speed in a no boundaries environment. Be that as it may, sound does not propagate at the same speed everywhere in underwater environments. In fact, sound speed depends on salinity, temperature and depth. To understand sound propagation in a certain environment, one has to determine the sound speed profile function of the previous elements. Moreover, in real-life scenarios, sound propagates between two boundaries: the surface and the bottom. In this regard, when an incident sound wave meets a boundary, it will partly reflect and transmit through the interface (depending on the boundary it may be one, the other or both).

Moreover, when considering passive acoustic monitoring (PAM), one should realize that sound is composed of signals, noise and interferences. Noise and interference are unwanted signals that hamper the capability of recognizing the signal of interest. In fact, noise is considered to be a randomly varying signal. Ambient noise can be added to the signal, but also self-noise in case the system used makes noise itself.

2- Cetacean sounds

This section introduces the sound and signals of interest of the project: cetacean sounds. Cetaceans use sound for many purposes: echolocation, communication, foraging, etc. They therefore generate a large variety of sounds. The easiest and most common way to depict cetacean sounds is to plot the sound pressure as function of time. Hence, classification of these sounds is related to the acoustic appearance of the emitted signal, in time and in frequency. Cetacean sounds are conveniently divided into two categories: echolocation “clicks” and “communication signals”.

i - Communication signals

Communication is the most obvious use of sound for underwater mammals. Typical communication signals are whistles or complex call sequences. They are relatively tonal or pulsed signals with a varying degree of spectral variability and with potentially low directionality.

In a noisy or complex environment, the transmitted signals’ complexity may be increased in order to convey the information to the receiver. If this approach fails for a very long-range communication, the cetacean may slow down the information rate and transmit very simple signals over long periods of time. Therefore, these communication signals seem very unpredictable for the human being. Furthermore, the signals depend on the type of communication and the information conveyed. Not all types of cetacean communications are fully understood yet.

ii - Echolocation signals

Echolocation is the use of sound by an animal to locate himself or an object, with the reflected sound wave of the emitted sound. For sea mammals, angular estimation may be done with an omnidirectional transmitter and a directional receiver, the angular resolution being limited by the distance between the ears.

Communication signals being complex, scientists use more commonly these echolocation clicks to study cetaceans, their behavior as individuals and in a group. For instance, the clicks emitted by beaked whales when they dive enable one to locate them. Clicks are directional short time pulses of highly significant intensity. In this regard, we will focus in this project on echolocation clicks to locate cetaceans. We will therefore deliberately overlook communication signals. The first step is to detect these clicks.

B - The environment and the means of interest of the experiment

In this part, we may depict the environments, the sounds and the means of interest for the experiment in order to determine a specification. In this regard, the Azores waters will be the topic of the study to understand in which environment we have been simulating the localization methods. We may in

parallel develop the environment off Cabo Espichel where the tetrahedron array was actually placed. At last, we will develop the AUVs of the experiment to dimension the hydrophone locations.

1 - The Azores' and Lisbon's environment

The Azores is an archipelago composed of nine volcanic islands in the North Atlantic off Portugal's coast (38.6°N 28°W). This area is particularly interesting for its seabed and its underwater wildlife. It is the largest cetacean sanctuary in the world with 27 identified species. The area of the second experiment off Cabo Espichel was chosen because it is situated just after the continental shelf of Portugal, in deep waters.

i - The depth of the environment

In order to describe the underwater environment, we first needed to determine the shallow or deep-water scenario. In this matter, we simulated (figure 1) the seabed of the Azores according to an available global bathymetry database via GEBCO (General Bathymetric Charts of the Oceans). This figure focuses on the area around Faial and Pico, the two main islands to the south of which there is the highest concentration of cetaceans.

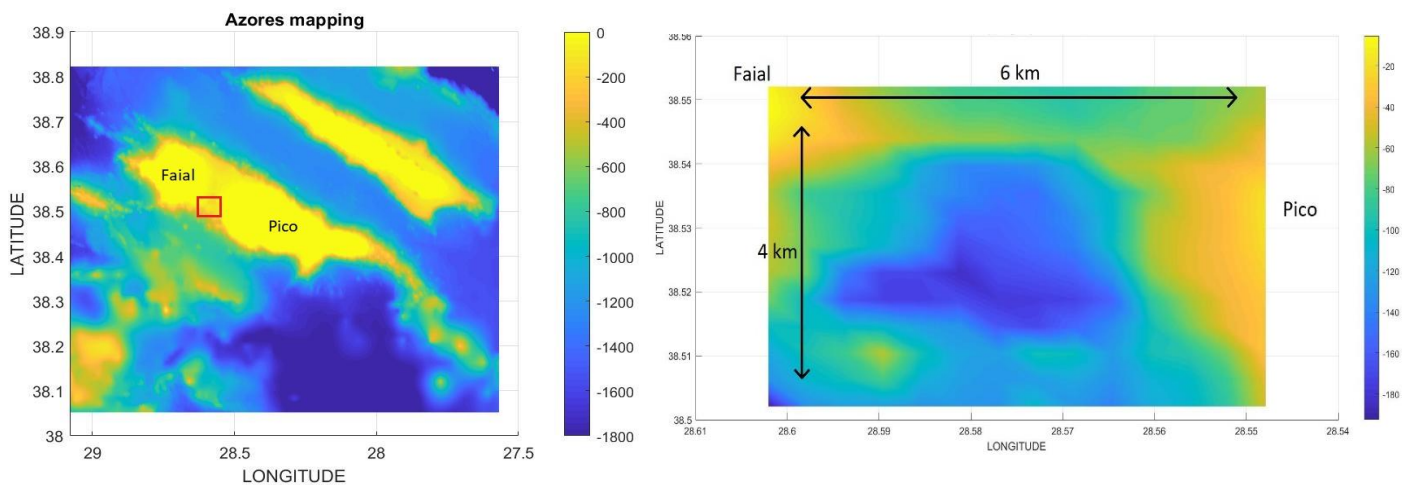


Figure 1 - Mapping of the Azores (left panel) and of the area of interest (right panel)

The area of interest for the experiment is between the islands of Faial and Pico as shown on figure 1. It represents an area of 24 km^2 with bottom depths up to 160 m. In account of the area of interest and its respective depths, we may consider that the cetaceans are progressing in shallow waters.

Figure 2 pictures the mapping of the seabed off Cabo Espichel. One may notice that the experiment was conducted just after the limit of the 200 m deep continental shelf, above a depth of 2000 m. The depth of the seabed in the area can go up to 2500-3000m. The array being hung at a depth of 80 m, we may consider that the cetaceans evolve in deep waters and not in shallow waters as in the Azores.

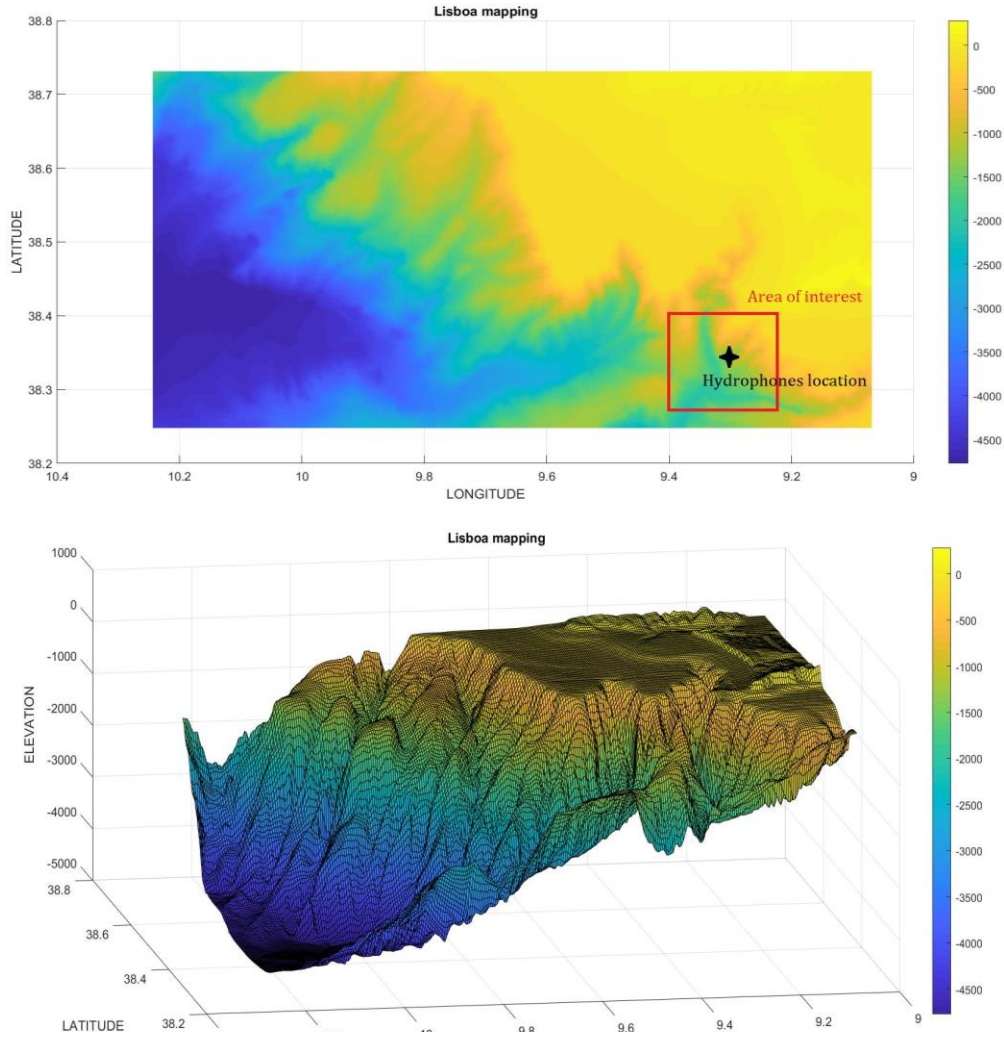


Figure 2 - Mapping off Lisbon's coast (upper panel) and of the area of interest (lower panel)

ii - The sound speed profile (SSP) of the environment

In order to study the underwater acoustic propagation scheme, one needs to know the sound speed profile (SSP) of the area of interest. Indeed, the knowledge of the SSP enables one to understand the path taken by the acoustic rays and may help to make some hypothesis depending on the methods of localization used.

SSP depends of three parameters: temperature (T in $^{\circ}\text{C}$), salinity (S in psu) and pressure (p in Pa). We may note that depth is directly related to the pressure. To calculate the SSP of interest in the two studied environments, we used a global database from the National Oceanic and Atmospheric Administration (NOAA) World Ocean Atlas available on the internet.

$$c = 1449.2 + 4.6 * T - 0.055 * T^2 + 0.00029 * T^3 + (1.34 - 0.01 * T) * (S - 35) + 1.58 * 10^{-6} * p \quad (1.4)$$

With these data and using the Mackenzie underwater sound speed equation (1.4), we were able to draw with the software Bellhop the two SSPs we needed (figure 3 and 4).

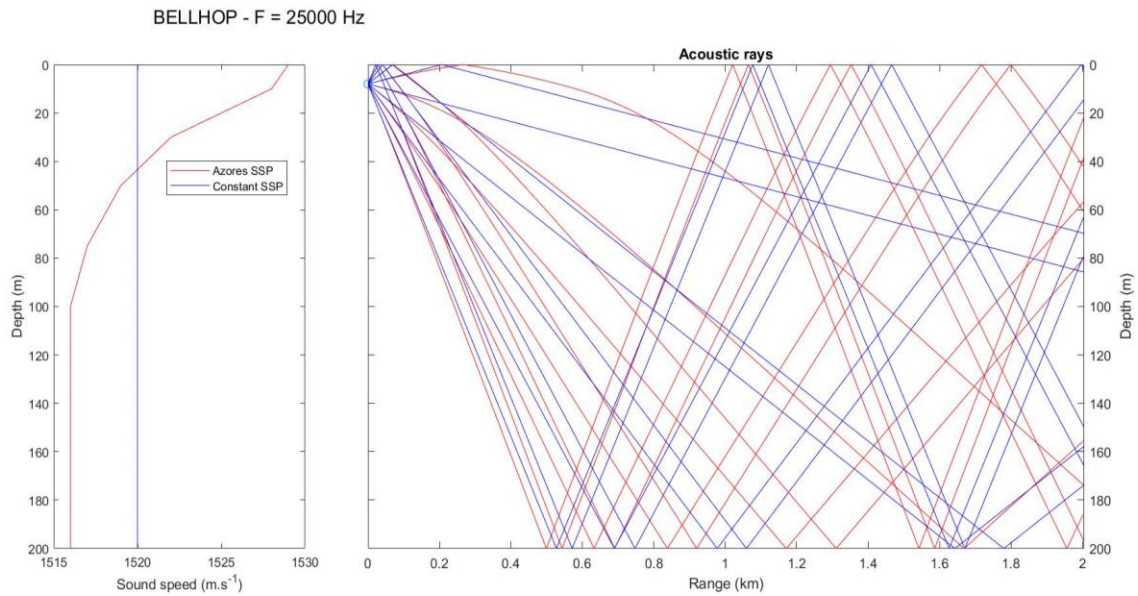


Figure 3 - SSP and ray paths of the Azores compared to a constant SSP

Figure 3 shows the SSP of the area of interest in the Azores (in red), compared to a constant SSP (in blue). The source is situated at a 8 meter depth on this graph. Yet, the ray paths being the same back and forth, we may swap the receiver and the transmitter and consider that the receiver (the hydrophones) is placed at a 8 meter depth. It is notable that in shallow waters, many reflections upon the surface and the bottom occur and that the energy of the received signal after some reflections may be attenuated. We may also observe that for direct path rays there is a distance difference between the two SSPs.

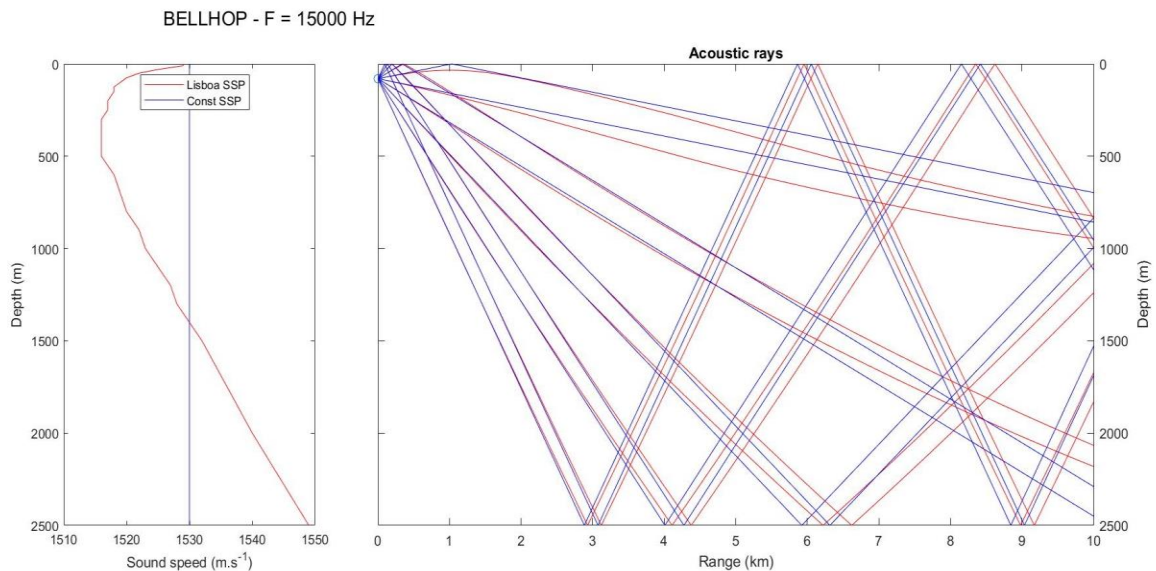


Figure 4 - SSP and ray paths off Lisbon's coast compared to a constant SSP

As for figure 4, Cabo Esbichel's SSP is compared to a constant SSP. Taking into account depth in this area we are no longer in the field of shallow waters. As we can see on figure 4 interaction with surface and ground are much less numerous and appeared at much higher distance that in the Azores' graph. Contrary to the Azores we may see that the hypothesis of constant speed is applicable over greater distance and with expected localization results closer to reality.

2 - The means: AUVs

Underwater gliders are autonomous vehicles with very low power consumption that propel themselves through the ocean for a long period of time over a long distance. In this part, we will present and describe the AUVs that were meant to be used for the PAM experiment in the Azores. Nevertheless, we will not develop all the details concerning the programming of the AUV and the glider operation given that it is only a tool for our project and our experiment.

i - Slocum glider

This AUV is not meant to be used for the JONAS project but enables one to understand the complexity and the current interest of scientists in underwater gliders. Slocum gliders are AUVs that do not use traditional propellers and thrusters, but variable-buoyancy propulsion to glide forward. In this regard, the slocum glider uses the variation of their ballasts added to their hydrofoil wings to convert a vertical movement into a horizontal movement: the glider dives with a constant angle to the bottom and rises to the surface likewise. Without any need of human operator guidance, these AUVs can travel very long distances by using hardly any energy. They navigate with the help of different navigation tools (pressure sensors, magnetic compasses, periodic surface GPS fixes, etc.) enabling the collection of positional information. Underwater gliders are used for many purposes, going from environment measurements to PAM. For each use of an underwater glider, a mission program is decomposed into three steps: the heading (the glider uses a tail rudder to adjust its course), a dive profile (the two depths between which it can operate) and a mission duration (from the first dive to surfacing).



Figure 5 - Example of a slocum glider diving profile (source: *Equipping an underwater glider with a new echosounder to explore ocean ecosystems*, K. J. Benoit-Bird)

ii - Wave glider

The type of AUV used for the JONAS experiment is a wave glider [10]. The wave glider can be separated into three parts as shown on figure 6: the float, the umbilical cord and the glider. The float contains all the recorders and batteries needed for the experiment plus solar panels. The float is sensitive to the wave movements and captures the wave's energy that it transmits via the umbilical cord to the sub. Similarly to the glider, the wave glider's sub has an underwater sinusoidal track between two depths. It

is therefore the wave's energy that propels the AUV and not the buoyancy. Contrary to the left panel of figure 7, the wave glider of the experiment does not carry any propeller or rotor.

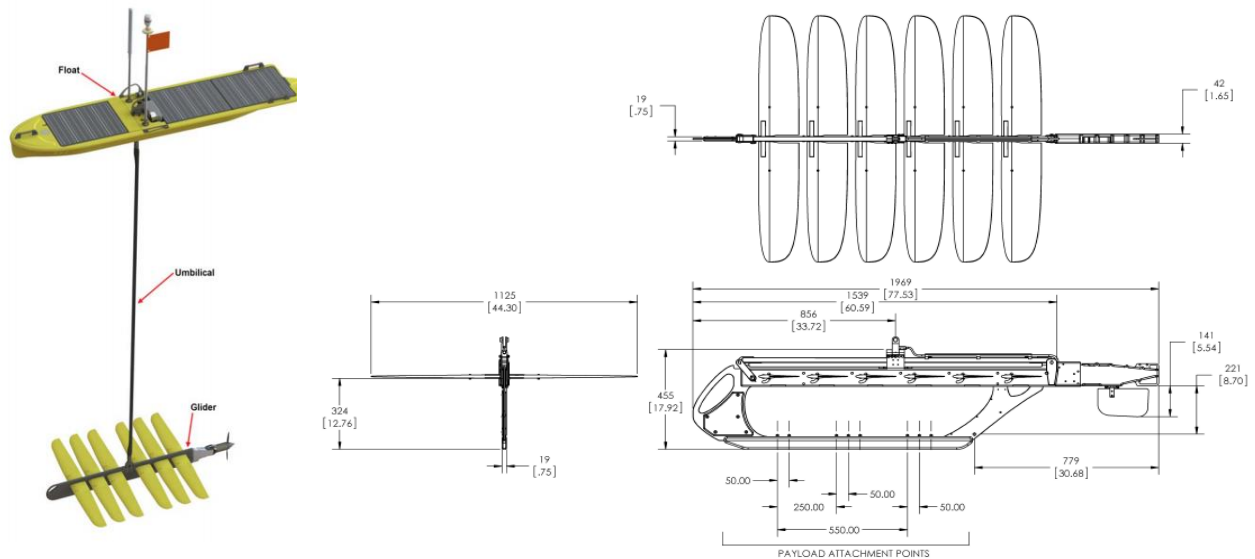


Figure 6 - Wave glider (left panel) and the overall dimensions and attachment points (left panel)
(intern source)

The absence of a propeller or constant spinning rotor enables the underwater glider to be acoustically quiet. Nevertheless, the wave glider may be subjected to noise coming from the floater sailing through the waves given that the sub is close to the surface (or when changing buoyancy for the slocum). Furthermore, the AUV does not emit any bubbles which would contribute to self-noise, contrary to ship-based echo sounders and towed arrays.

Underwater gliders seem to be an interesting choice regarding their very advantageous low acoustic signature, their autonomy and the distances travelled. However, like every AUV, underwater gliders have to cope with some constraints. Here, the array of hydrophones is spatially constrained to the glider's dimension [14]. In fact, in accordance with figure 6, the frame beneath the sub is the payload attachment points of the hydrophones and does not exceed one meter. In this regard, the hydrophone array will have to be « small ». The last constraint is the AUVs' depth. For the slocum glider, depth boundaries can easily be chosen and the AUV may evolve in deeper waters. Nevertheless, the wave glider is limited to the umbilical cords' length *i.e.* 8 meters. Finally, one has to record the diving angle and orientation of the sub in order to apply these pitch-roll-yaw corrections to the calculated source location. Be that as it may, other problems can be dealt with the programming of the different hydrophones.

C - Simulation of the target

The preparation of the experiment included cetacean signal simulation. For this purpose, we decided to simulate echolocation clicks for a certain type of cetacean that is present in the Azores: the beaked whale. We may note that the simulated signals can be applied, with different characteristics, to other cetacean echolocation signals.

1 - The sound source: the beaked whale

First, we decided to study a particular type of cetacean massively present in the Azores and easily identifiable with echolocation clicks. In this way, we have chosen to study the beaked whale.

i - The beaked whale specie

The Ziphiidae family *i.e.* the beaked whale family is made up of at least 22 different species. Little is known about this family because of the low abundance of these mammals and their offshore deep-water habitat. They tend to flee ships and boats and are therefore difficult to observe. Furthermore, they do not spend much time at the surface to breathe (about 8% of the time has been reported). The beaked whale family is a widespread family in all the oceans and is known to congregate in deep waters off the continental shelves. The beaked whale is a deep diver, diving regularly to depths exceeding 500m. These extreme dives are related to foraging for these mammals. In this regard, they echolocate their food by emitting clicks. Many studies have proven that the human impact of ships and active SONARs hamper the behaviour of the Ziphiidae family: the cetacean tends to dive deep in the ocean and flee the noise emitted by human activity. That underscores the importance of PAM for studying beaked whales: detect and localize cetaceans without hindering their attitude.

ii - Beaked whale echolocation signals

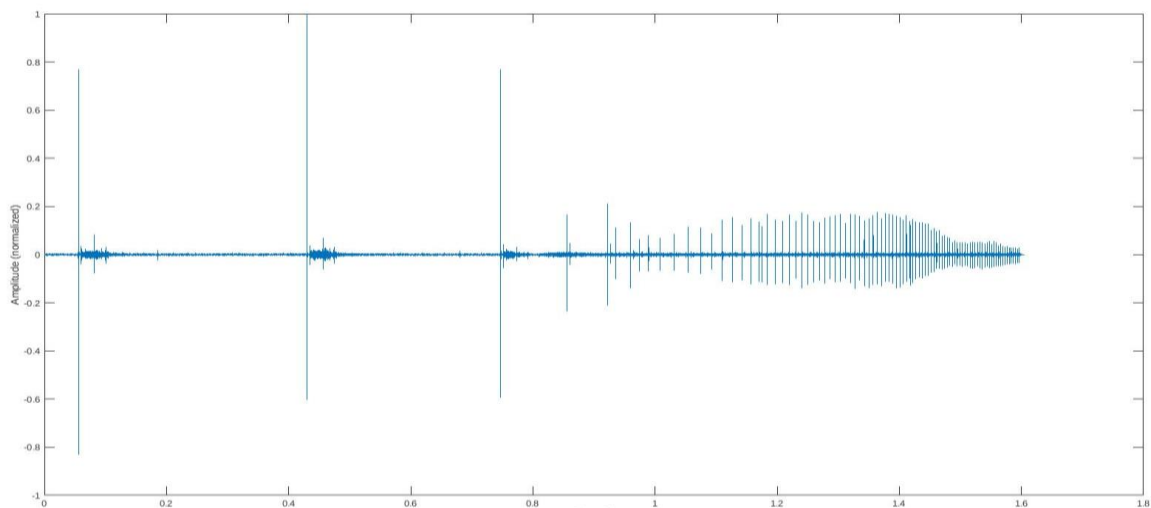


Figure 7 - Time domain beaked whale clicks (source: intern source)

As shown above in figure 7, a sequence of a Cuvier's beaked whale clicks is presented. Each sequence of click is specific to a different species. Studying the characteristics of the clicks may help to determine the nature of the detected cetacean. The graph highlights the fact that until 0.9s, the emitted clicks are emitted around every 0.2 to 0.4 seconds. This time length is called the Inter-Click Interval (ICI). These types of clicks are called search clicks. Afterwards, the ICI diminishes and many clicks are emitted in a short amount of time. As a matter fact, the sequence after 0.9s corresponds to the moment when the whale is close to the food and starts to multiply echolocation clicks which are called buzz clicks. We will not focus on that part of the scope but on the « diving echolocation », that is to say the search clicks, because they are detectable closer to the surface and they are emitted all the way through the diving sequence.

2 - Numeric simulation of the sound source: beaked whale clicks

Many species exist in the Ziphiidae family (Cuvier's beaked whale, Blainville's beaked whale, Gervais' beaked whale, etc.). Each type of beaked whale click has different characteristics that can help to classify and identify the detected cetacean [12].

i - Different characteristics of the beaked whales' clicks

In figure 8 below, the waveforms and spectrograms of several beaked whales are depicted. These results were obtained during an experiment in the western Atlantic Ocean where various beaked whales were detected via PAM systems in 2016. During this experiment, cetacean sounds were recorded in six different locations off the entire North American coast. We can see that each click has some similarities. Indeed, the time domain of the clicks shows that the waveform of each click looks similar. Likewise, the spectrograms show that the energy is concentrated in a small area of the spectrogram.

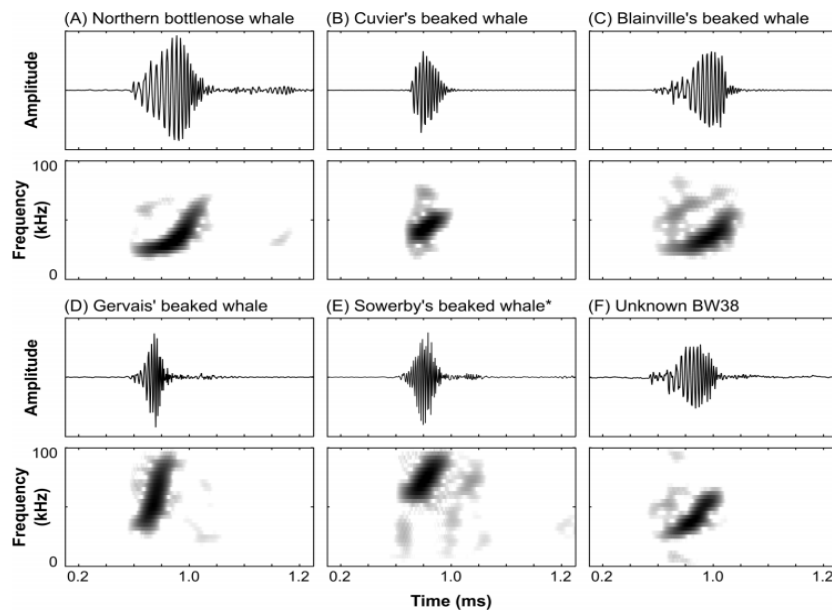


Figure 8 - Examples of waveform (upper panels) and spectrograms (lower panels) of different beaked whales (source: NRC research press, *Using passive acoustic monitoring to document the distribution of beaked whale species in the western North Atlantic Ocean*, Joy E. Sanistreet)

ii - Click generator simulation

Recorded beaked whale signals being complex to exploit at first (noise presence due to the environment for example), we chose to simulate beaked whale clicks ourselves. In order to simulate the signal received by a four-hydrophone array, we first needed to choose an emitted signal. With MATLAB, we created a click simulator of three clicks in which for each click, we could choose:

- the ICI ;
- the pulse length t_{click} ;
- the bandwidth of the click $[f_0, f_1]$;
- the peak location t_{peak} ;
- the peak frequency f_{peak} ;

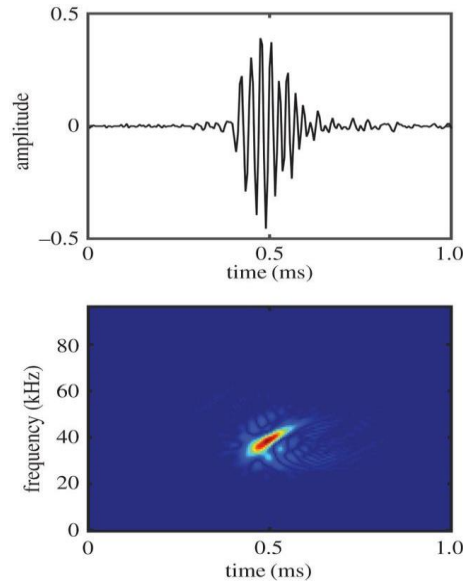


Figure 9 - Cuvier's beaked whale clicks' waveform (upper panel) and spectrogram (lower panel) extracted from the 2013 towed hydrophone array data (source: *Beaked whales demonstrate a marked acoustic response to the use of shipboard echosounders*, Danielle Cholewia)

We relied on known data about Blanville's beaked whale search clicks as shown above on figure 9. This data was obtained between 2011 and 2013, when broad-scale cetacean assessment surveys were conducted as part of the Atlantic Marine Assessment Program for Protected Species (AMAPPS). The ICI is typically between 0.2 and 0.4s. The clicks have a distinctive form of an FM upsweep with a -10 dB bandwidth of [26,51] kHz and a pulse length of 200 μ s. The spectrogram of the figure 10 represents a linear distribution of the energy between 35 and 42 kHz on the period [0.45,0.55] s. To simplify our study, we decided to use a simple spectrogram distribution around the peak frequency of the click. We considered a bell-shaped envelope for the waveform with a gaussian function:

$$p(t) = \text{Re}(A \cdot e^{2if_{peak}t} \cdot f(t, t_{peak}, \sigma^2)) \quad (1.5) \quad f(t, t_{peak}, \sigma^2) = \frac{1}{\sigma\sqrt{2\pi}} \cdot e^{-\frac{1}{2}\left(\frac{t-t_{peak}}{\sigma}\right)^2} \quad (1.6)$$

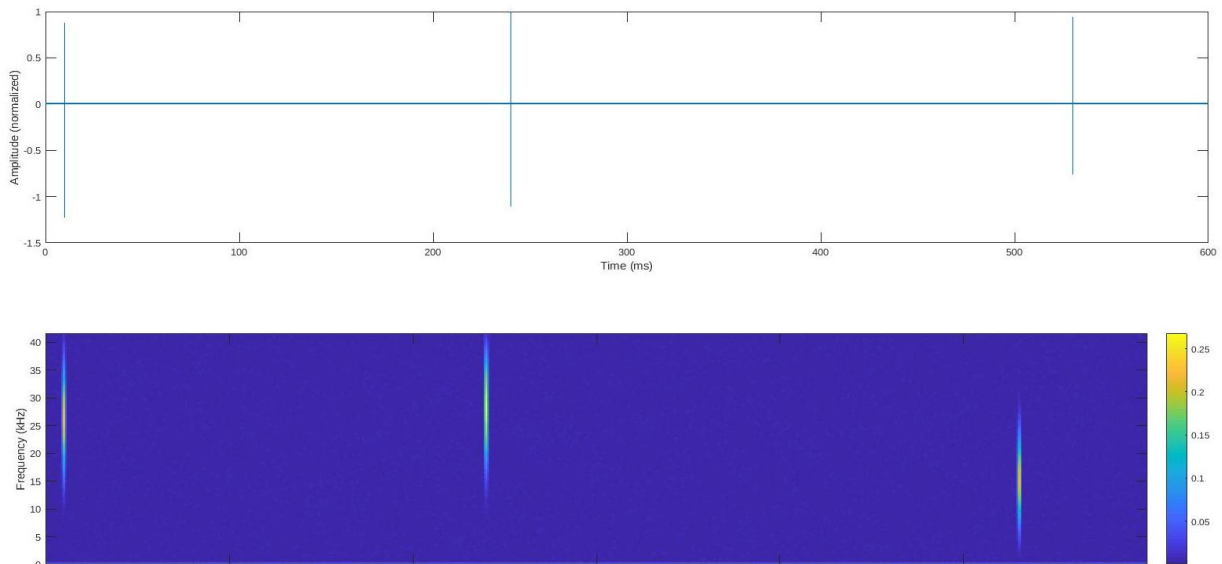


Figure 10 - Waveform and spectrogram of three simulated clicks

For the simulation of figure 10, we considered the following data for a three-click generator over 0.6s:

- $ICI = [230,290] s;$
- $t_{click} = [160,180,200] \mu s;$
- $[f_0, f_1] = [25,50] kHz;$
- $t_{peak} = [10,240,530] ms;$
- $f_{peak} = [57,55,68] kHz;$

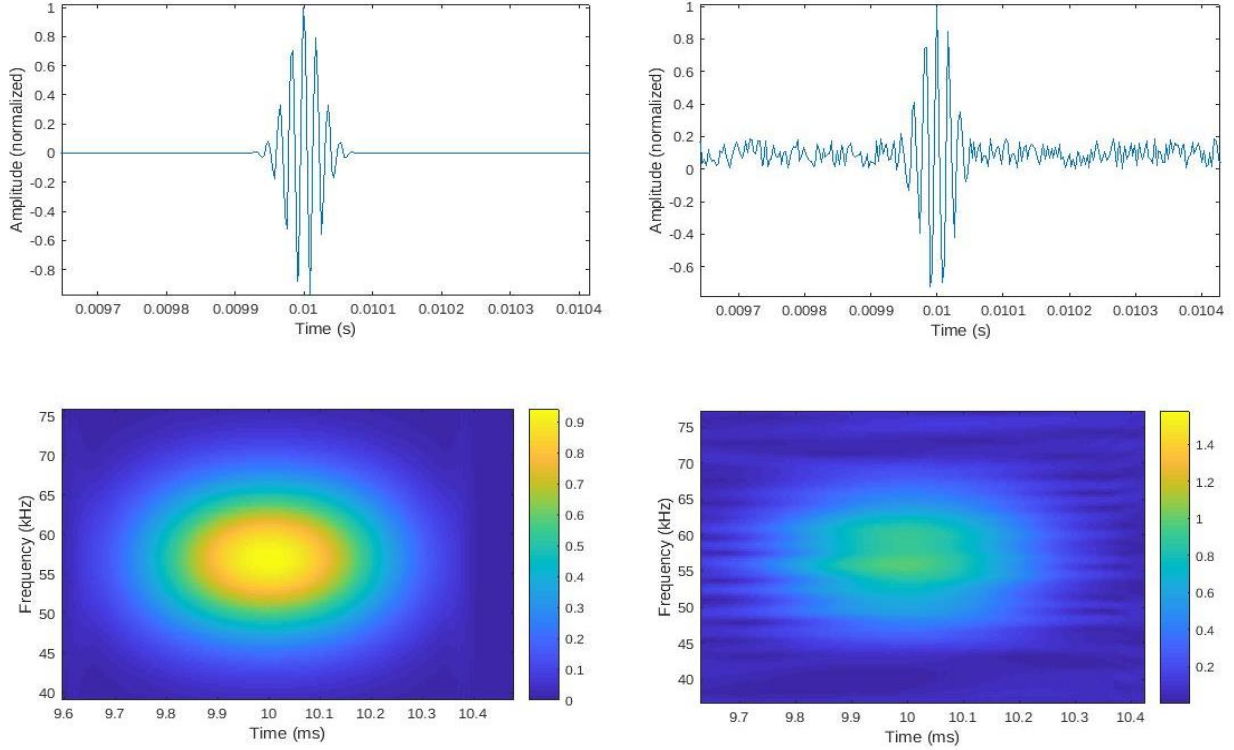


Figure 11 - Simulation of the waveform (upper panels) and spectrogram (lower panels) of one emitted click signal (left panels) and of the received signal by a hydrophone (right panels)

A zoom onto the first click gave us the figure 11 above. We can see that the energy is concentrated as chosen to coordinates of $[t_{peak}, f_{peak}]$, that is to say $[10 ms, 57 kHz]$. The left panel depicts the signal emitted by the source, whereas the right panel may be seen as the signal received by the hydrophones. In this effect, the received signal is a time delayed signal of the original emitted sound to which is added random noise (in accordance with a Gaussian function): $noise = A \cdot f(t, 0, 1)$ (1.7) where A is the amplitude of the noise.

II - Methods of localization for a four-hydrophone planar array

The context being set up, localization issues may be studied. In this regard, we will first expose the idea of signal detection and filtering in order to measure information of interest such as time difference of arrival (TDOA) between several hydrophone channels. Then, two different localization methods, direction and depth estimation, will be explained and simulated with the established context and environment. The studied methods are extracted from the work of Walter M.X. Zimmer, *Passive Acoustic Monitoring of Cetaceans* [13]. Numerical simulations of these methods were led afterwards.

A - Signal detection methods and time of arrival measurement

1 - Detection

Detection consists in defining for a recorded data if a transient of interest should be considered as a signal or as noise fluctuations, which are of no interest for PAM application [6]. Here, it is about telling for a certain frequency or amplitude variation if it corresponds to the presence of a marine mammal. Moreover, detection establishes also the selection of a method for reducing unrelated noise content by spectral filtering.

Generally, a simple detection method entails the insertion of a simple threshold to filter the low noise and to improve the sound to noise ratio (SNR). However, the areas of interest (Azores and Lisbon) are subjected to large human activity noise. Indeed, Lisbon shelters Portugal's' biggest trade and leisure harbour, whereas the Azores hosts many whale-watcher ships and fishing vessels. These activities contribute to the recorded noise level and can be detected as well as cetacean sounds. Thereby, noise makes marine mammals' detection difficult.

A more efficient method for our study relates to frequency studying. Indeed, a major part of this parasitic noise focuses on low frequencies ($< 1 \text{ kHz}$ generally), whereas cetacean frequency scope copes with higher frequencies and a larger bandwidth spectrum. Thereby a sorting of the samples can be done with a filtering operation, a spectrum analysis or a combination of both. It then becomes possible to select samples where the appearing information interests us to detect mammals' presence.

2 - Measurement of time difference of arrival: cross-correlation

A single hydrophone measures the pressure in the water in order to detect signals. It can therefore detect sounds coming from a source but cannot localize it on its own. One needs more information to determine where the signal comes from. In this regard, arrays of several hydrophones may be used. As a matter of fact, each hydrophone receives a similar signal, to which noise is added, at a different time. This time difference of arrival (TDOA) between two hydrophones is an additional information that can enable one to localize the sound source (in bearing, depth or range) [1]. Consequently, we need a measurement of the arrival time difference in a pair of hydrophones.

A common method to determine the TDOA between two hydrophones is the cross-correlation method. Cross-correlation is a function which permits to measure the similitude between two signals and determine relative delay by finding the lag time where the function is maximal. TDOA estimation by means of cross-correlation works best if the two signals have distinctive temporal and spectral features. As shown by (2.0), it consists in fixing time for one of the signals and shifting the second signal in the time domain to compare it to the first one.

$$\Gamma_{ab}(\tau) = \int_{-\infty}^{+\infty} a(t) \cdot b(t - \tau) dt \quad (2.0)$$

Knowing the instant when the absolute value of this cross-correlation function is maximum enables one to find the instant when the two signals are most similar. By applying that on signals received on different hydrophones this instant becomes the TDOA.

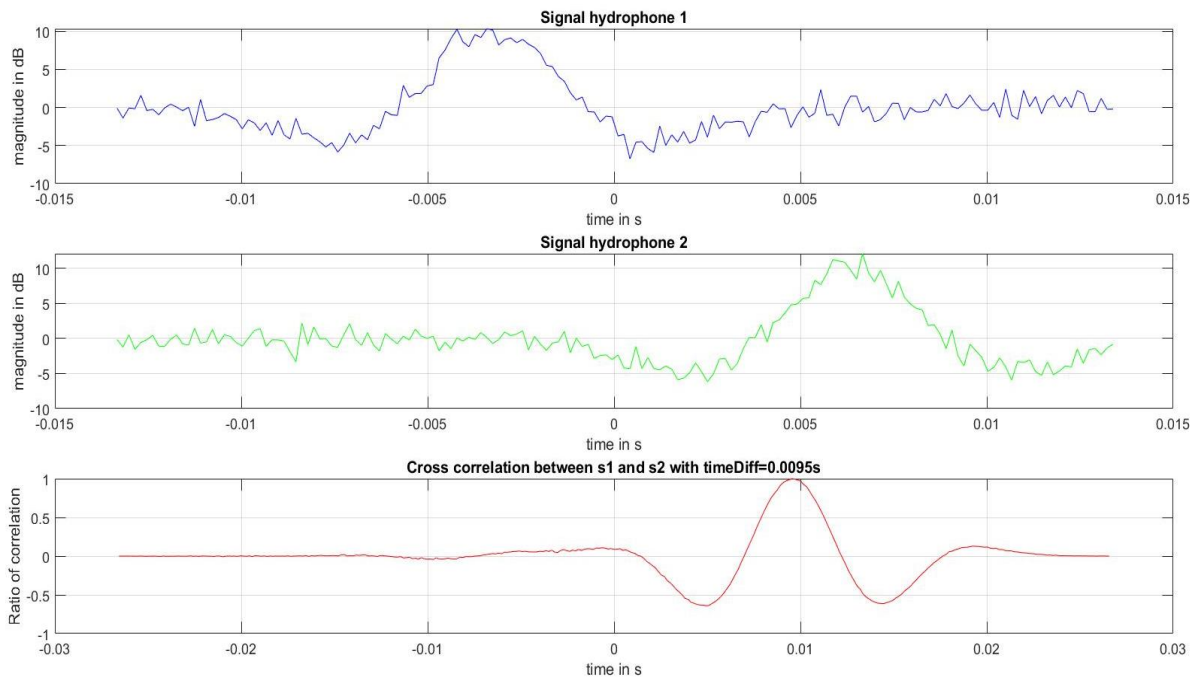


Figure 12 - MATLAB cross-correlation simulation with two delayed noisy Ricker signals

As an example, the figure 12 above represents two time-delayed Ricker signals received with different additive noise by two different hydrophones (two upper panels). The lowest panel depicts the cross-correlation function in the time domain of the two previous signals. The maximum of the function then corresponds to a $TDOA = 9.50 \text{ ms}$, which is coherent with the time-delay implemented into the Matlab program. Although the noise is random, it does not affect the cross-correlation function as the maximum correlation ratio is equal to one.

Nevertheless, time delay estimation with cross-correlation may be very time-consuming depending on the sampling frequency and the distance between two hydrophones. This may be an issue for a high sampling frequency and widely spaced hydrophones. Furthermore, the minimum distance between two hydrophones must be over half of the signals' wavelength for the resolution. Considering a frequency $f = 55 \text{ kHz}$ and a sound speed $c = 1520 \text{ m} \cdot \text{s}^{-1}$, the distance between the hydrophones must be at least $d = 2.8 \text{ cm}$. In this regard, the distance between each hydrophone for our experiment is not an issue considering the dimensions of the wave glider.

B - First method of localization: bearing estimation (direction finding)

1 - Azimuth and elevation finding method

In this part, we will develop a method of coplanar arrays requiring at least three hydrophones for a two-dimensional direction finding. This method of direction finding is based on the TDOAs measured between pairs of hydrophones. We will consider only the direct ray paths of the emitted sound for each hydrophone. Thus, a bearing finding between two hydrophones can be extended to three hydrophones and more in order to localize in two dimensions.

i - Direction finding with a hydrophone pair

The simplest method to find a source bearing is to use two hydrophones and measure the time difference of arrival of a signal emitted by a source S . For distant sources, closely spaced hydrophones are sufficient to estimate the sound source bearing. Considering a pair of hydrophones H_0 and H_1 receiving sound from a distant source location S as shown on figure 13, one may establish the following formula:

$$R_1^2 = R_0^2 + L_1^2 + 2R_0 L_1 \cos\beta \quad (2.1)$$

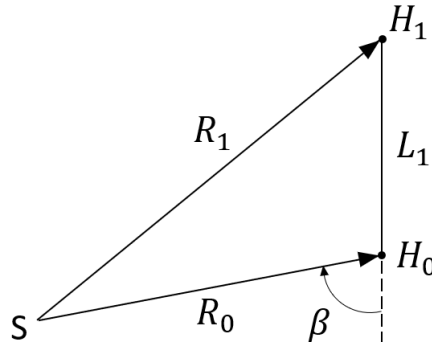


Figure 13 - Estimation of sound arrival angle

In this case, we will estimate the arrival angle β , noting that there is a rotational symmetry, the same angle β being obtained by flipping the whole figure to the right. To obtain this arrival angle β angle the hydrophone H_0 , we may denote the sound path difference $\delta R_{10} = R_1 - R_0$:

$$\cos\beta = \frac{\delta R_{10}}{L_1} + \frac{L_1^2 - \delta R_{10}^2}{2R_0 L_1} \quad (2.2)$$

For very long ranges, i.e. $R_0 \gg L$ and $R_0 \rightarrow \infty$, and with the relation $\delta R_{10} = c\delta\tau_{10}$, where $\delta\tau_{10}$ is the TDOA between the hydrophones H_0 and H_1 , (2.2) becomes:

$$\cos\beta = c \cdot \frac{\delta\tau_{10}}{L_1} \quad (2.3)$$

Moreover, considering a distant source, $R_0 \rightarrow \infty$ is equivalent to assuming that the sound reaches both hydrophones with the same angle, i.e. the sound may be described as a plane wave.

ii - Two-dimensional constrained direction finding with a three-hydrophone array

Three hydrophones always describe a plane in a three-dimensional space. Thereby, the direction finding relies on the ambiguity that the side of the plane from which the sound truly comes from is not known. With a three-hydrophone array, there are two possible bearings. We may consider another hypothesis to counter this issue: a horizontal plane three-hydrophone array close to the surface (case of the wave glider). In fact, regarding the depth of the fixed hydrophones (maximum 8 meters) and of the target *i.e.* deep diver cetaceans such as beaked whale, this hypothesis may be taken into account in the framework of our study if we consider the direct path rays coming from under the array.

Given three hydrophones H_i ($i = 0,1,2$) placed at the coordinates (h_{ix}, h_{iy}, h_{iz}) , we may define two vectors d_1 and d_2 and the associated distance L_1 and L_2 between the hydrophones, where $d_i = h_i - h_0$ and $L_i = |d_i|$. Only hydrophones H_0 and H_1 are shown on figure 14. Furthermore, as depicted on the figure, direction finding is equivalent to searching for the azimuth γ_i between two hydrophones and the elevation ϑ knowing the previously calculated angle β_i (cf II.A.2.i). We can add the angle ω_{12} between the vectors d_1 and d_2 : $\omega_{12} = \gamma_1 + \gamma_2$ (2.4).

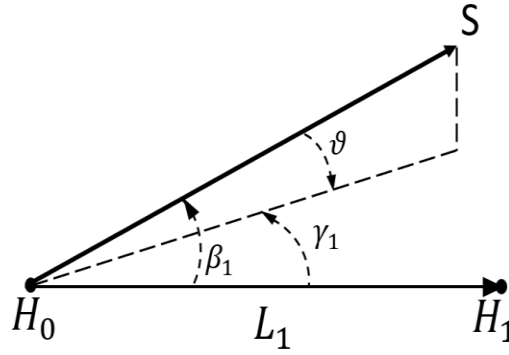


Figure 14 - Angles for two-dimensional constrained direction-finding

Following the figure above, we express the directional cosines as:

$$\cos \beta_1 = \cos \gamma_1 \cdot \cos \vartheta \quad (2.5)$$

$$\cos \beta_2 = \cos \gamma_2 \cdot \cos \vartheta \quad (2.6)$$

By equations (2.4) and (2.5) in equation (2.6), we obtain: $\cos \beta_2 = \cos (\omega_{12} - \gamma_1) \cdot \frac{\cos \beta_1}{\cos \gamma_1}$ (2.7)

$$\text{And therefore: } \cos \beta_2 = \cos \beta_1 \cos \omega_{12} + \cos \beta_1 \sin \omega_{12} \frac{\sin \gamma_1}{\cos \gamma_1} \quad (2.8)$$

$$\text{We can therefore estimate the azimuth } \gamma_1: \quad \gamma_1 = \arctan \left(\frac{\cos \beta_2 - \cos \beta_1 \cos \omega_{12}}{\cos \beta_1 \sin \omega_{12}} \right) \quad (2.9)$$

Likewise, the angle γ_2 may easily be calculated. The elevation angle ϑ is then estimated with equation (2.5) or (2.6). Here intervenes the “above or below plane ambiguity” given that ϑ may be either positive or negative. As mentioned above, this ambiguity can be countered by considering the sound arriving from below the plane array.

2 - Simulation of the method

As mentioned in part I, we dispose for the Azores' experiment of a wave glider and four hydrophones. The spatial constraint is to fix the four hydrophones directly onto the AUVs' frame. Given the shape of the wave glider and the attachment points, we decided to study a plane square geometry array. To fit the frame of the AUV, the simulation may be also applied to a rectangular plane array. According to the previous models, three hydrophones are sufficient enough to localize the sound source. Nevertheless, we applied this method with a fourth hydrophone to correlate and confirm the results. In this part, we may refer to some MATLAB scripts that may all be found in the appendix A.

i - Scheme of the numerical simulation

We programmed with MATLAB the previous method by placing the sound source that we simulated (part II.C.2.ii.) where we wanted it to be. In this effect, we first chose the spherical coordinates of the source ($\mathbf{r}, \gamma, \vartheta$), where \mathbf{r} is the range of the source in meters (m), γ the azimuth angle and ϑ the elevation angle in degrees ($^\circ$). We do not consider the depth of the array; the bearing of the sound source is related to the position of the array. We then simulated the signals received by each hydrophone given the location of the source (figure 12) with the program *signal_received_by_array.m* and programmed the direction-finding method to find back the location of the source. This method enables one only to find the couple (γ, ϑ) and not the range \mathbf{r} .

ii - TDOA measurement simulation

First, we programmed the TDOA measurement with the script *crosscorr_TDOA.m*. We added an ambient noise level of 5 to 10 dB. In order to evaluate the accuracy of cross correlation, we calculated TDOAs with cross correlation and compared it to the theoretical TDOAs (program *compare_TDOA.m*). In this sense, we fixed the range of the source (distant source) and calculated TDOAs for two different cases: (1) fixed azimuth - changing elevation and (2) fixed elevation - changing azimuth. The initial data implemented in the program is given by:

- distance between the source and the hydrophone H_0 : $r = 8000m$,
- sound speed $c = 1500 m.s^{-1}$,
- distance between two hydrophones $L = 0.5m$,
- position of the hydrophones: $H_0 = [0,0,0]; H_1 = [0, L, 0]; H_2 = [L, 0, 0]$,
- angle between the two pairs of hydrophones: $w = 90^\circ$,

Figure 15 pictures case (1) where the fixed variables are r and $\gamma = 40^\circ$ with varying elevation angle, whereas figure 16 depicts case (2) with the fixed variables r and $\vartheta = 40^\circ$ with varying azimuth angle. These simulations and results were obtained for one pair of hydrophones. On each figure is shown the theoretical TDOAs that are calculated knowing the exact source location, and the TDOAs calculated via cross correlation with the received signals. For each case, we made two simulations to calculate the TDOAs with cross correlation: before filtering (5 kHz high-pass) the signal received by the hydrophones (left panels) and after filtering (right panels).

For the referential of the spherical coordinates (or the γ, ϑ angles), given that we consider only the lower half-sphere to localize, we changed the elevation angle reference: $\vartheta = 0^\circ$ is placed on the horizontal axis (and not on the vertical axis) and the direction of rotation downward.

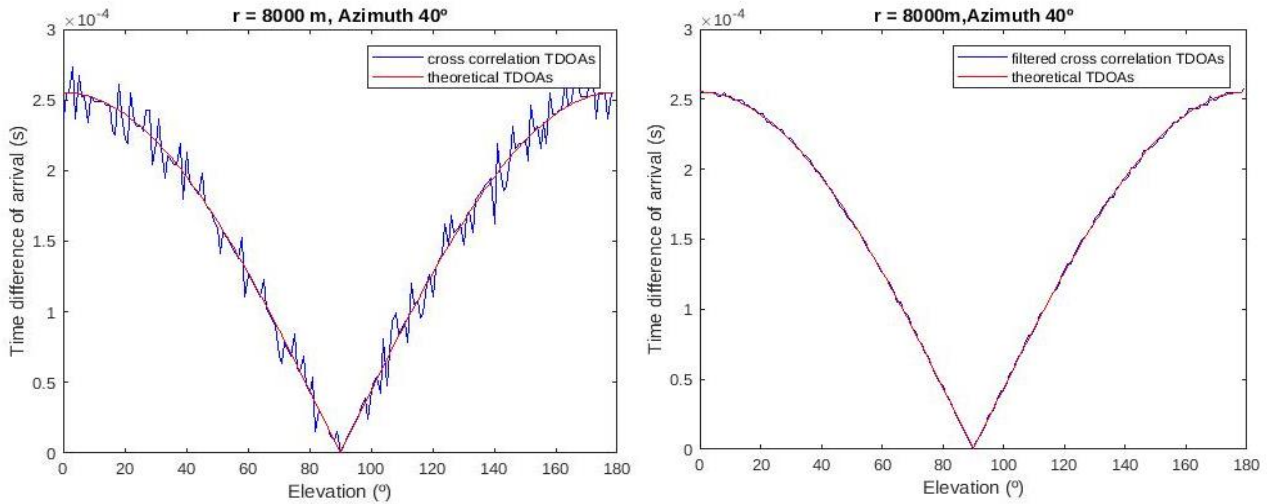


Figure 15 - Time difference of arrival for a fixed distance and azimuth in function of the elevation angle before (left panel) and after (right panel) filtering the received signal

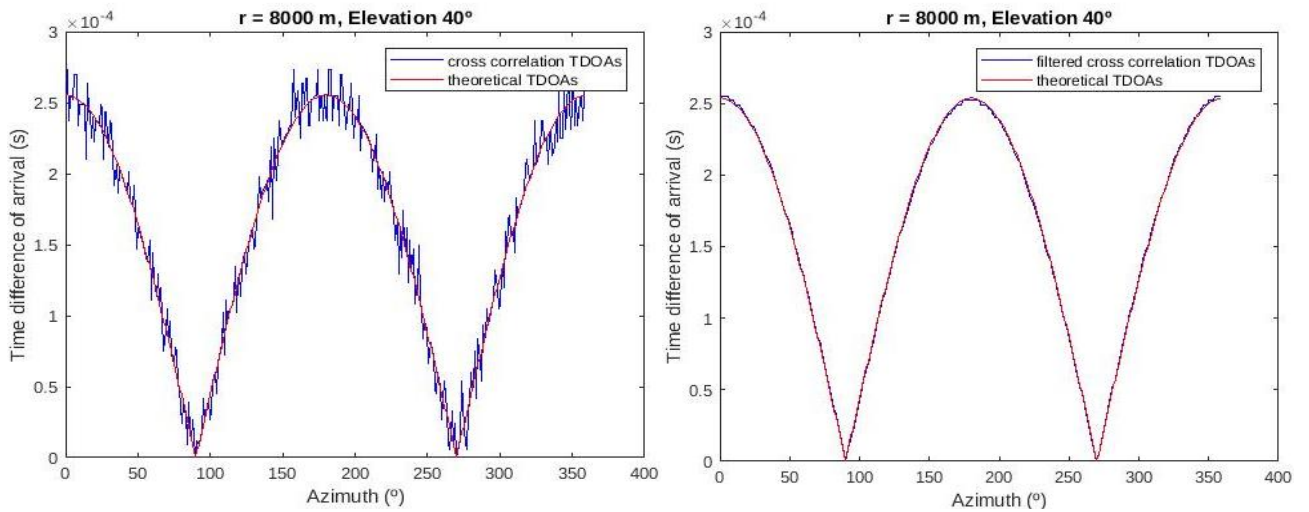


Figure 16 - Time difference of arrival for a fixed distance and elevation in function of the azimuth angle before (left panel) and after (right panel) filtering the received signal

It is notable that cross correlation gives us measurements that seem relatively close to the theoretical TDOAs. In this effect for the simulation of figure 15 (which applies similarly to the simulation of figure 16), the time difference between the theoretical and calculated TDOAs go up to $3,45 \cdot 10^{-5} \text{ s}$ when the signal is not filtered, whereas this difference is reduced to a maximum of $2,85 \cdot 10^{-6} \text{ s}$ in the case of the filtered signal. Thereby, we may note the importance of filtering the signal to obtain the most precise time of arrival measurements.

iii - Numerical bearing estimation

After measuring numerically the TDOAs, we simulated equations (2.9) to obtain the azimuth γ of the source and (2.5) to obtain the elevation ϑ of the source with the program *bearing_loc.m*. With the previous calculated TDOAs with simulated figure 17 (case (1) simulation) and 18 (case (2)).

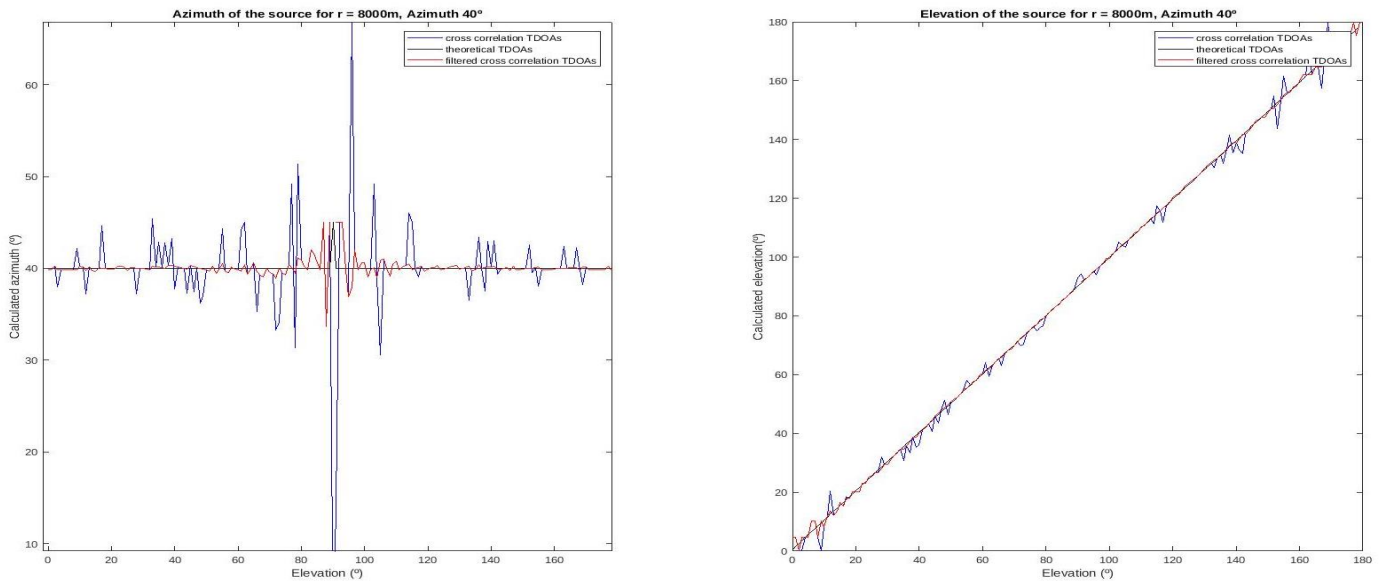


Figure 157 - Calculated azimuth (left panel) and elevation (right) for a fixed distance and azimuth in function of the elevation angle

As mentioned previously, the filtered signal gives more precise results in terms of TDOA measurements. Likewise, figure 17 stresses the more accurate estimated angles of the filtered signal. The right panel pictures the calculated elevation angle ϑ_c for a changing elevation ϑ . On the one hand, the non-filtered signal (in blue) can show up elevation angle errors up to 11° . On the other hand, the filtered signal (in red) shows up to 4° error in the band $[0,8^\circ]$ and $[172^\circ, 180^\circ]$, that is to say for small elevation angles, and up to 1.5° error in the rest of the band. Likewise, the left panel stresses on the accuracy of the method with a filtered signal. However, we may observe some peaks around $\vartheta = 90^\circ$ in all three graphic curves which does not correspond at all at the initial azimuth implemented into the simulation. The value of the peaks seem too inappropriate as the signal is not filtered. This peak may be explained as the source is directly underneath the array and the hydrophones receive simultaneously the signal and by looking at equation (2.5), $\cos \gamma_1 = \cos \beta_1 / \cos \vartheta$ with $\cos \vartheta \rightarrow 0$.

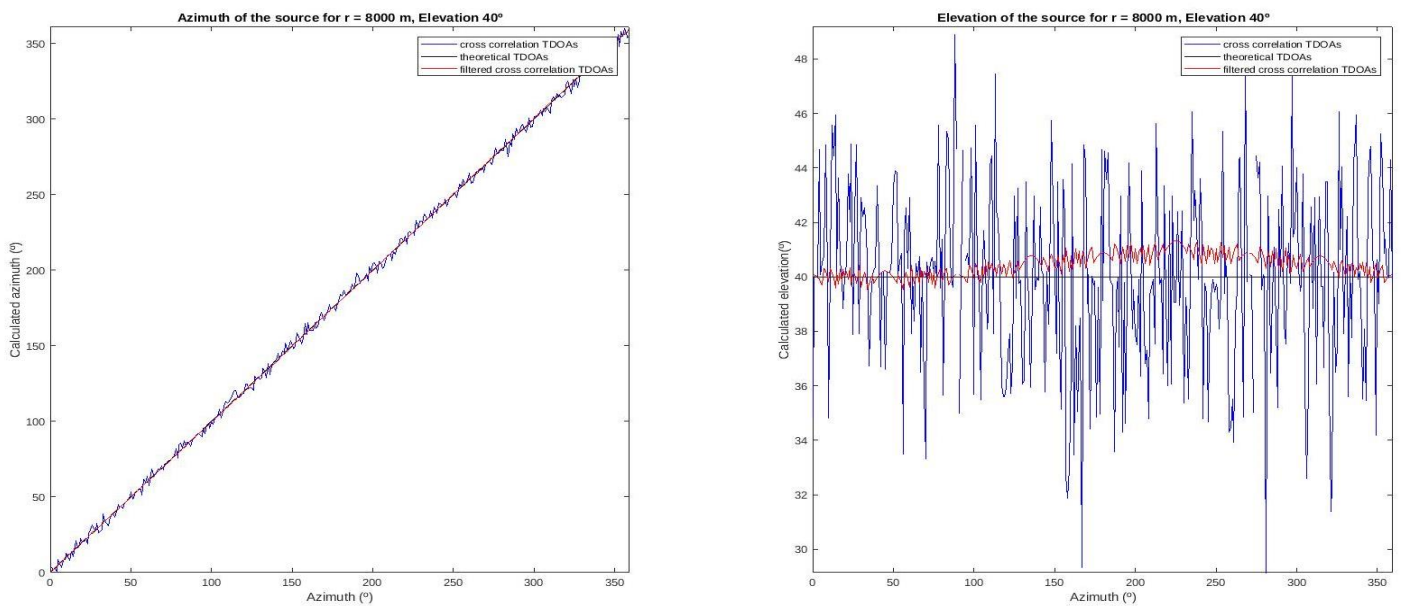


Figure 18 - Calculated azimuth (left panel) and elevation (right) for a fixed distance and elevation in function of the azimuth angle

As for case (2), highlighted by figure 18, one may observe that the comments made for the first case look alike. For a changing azimuth angle γ , the calculated azimuth γ_c (left panel) can bear an angle error of 10° in the case of the non-filtered signal, whereas the error does not exceed 1° on the case of the filtered signal. Moreover, the calculated elevation angle ϑ_c can show a difference of 12° for the non-filtered signal, and less than 1.4° for the filtered one.

From these numerical simulations, we may stress the necessity of filtering correctly the noise of the received signals on each hydrophone. Indeed, the value of the TDOA affects directly the value of the bearing of the sound source and one may find an error up to 10° in elevation and azimuth (in the presented case). Furthermore, one has to add some corrections to these estimated angles related to the orientation of the array and to the pitch-roll-yaw angles of the AUV. Before leading off the next localization method, these corrections are necessary in order to reduce the amount of errors.

C - Second method of localization: depth estimation

Another method consists in finding another parameter of the sound source localization, namely the depth of the source d . Yet, this presented method will need as entry variable a parameter measured with the previous method. Thus, this method is supplementary to the first one.

1 - Depth localization principle

The rays travelling the same way from the source to the receiver and the other way around, we can exchange the receiver and the transmitter and assume that the hydrophone H_0 is the sound source and S the receiver. We consider a hydrophone H_0 at the depth h , the sound source S at the depth d and two ray paths: the direct path and the surface reflected path. H_0 is at a distance R_0 from S . Considering the image above the surface $H_{0,s}$ of the hydrophone H_0 , we may depict the reflected ray path as a direct path emitted by the source $H_{0,s}$ at a distance R_s (figure 19).

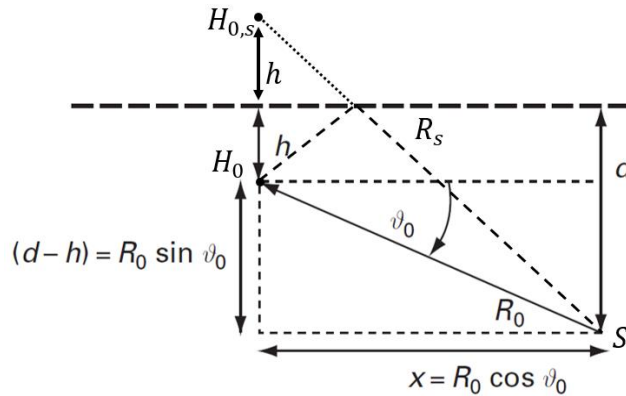


Figure 19 - Geometry and elevation angle ϑ

Given the angle ϑ_0 , one may obtain the following equation: $d - h = R_0 \sin \vartheta_0$ (2.11)

Using straightforward geometry, we obtain the set of equations:

$$R_0^2 = x^2 + (h - d)^2 \quad (2.12) \quad R_s^2 = x^2 + (h + d)^2 \quad (2.13)$$

The combination of equations (2.11) and (2.12) give us: $R_s^2 - R_0^2 = 4hd$ (2.14)

By considering the path difference between the direct and surface-reflected path δR_{S0} , where $R_S = R_0 + \delta R_{S0}$ and $\delta R_{S0} = c \cdot \delta \tau_{S0}$, with $\delta \tau_{S0}$ the TDOA between the two paths on one hydrophone, equation (2.13) becomes:

$$c^2 \cdot \delta \tau_{S0}^2 + 2 \cdot R_0 \cdot c \cdot \delta \tau_{S0} = 4hd \quad (2.15)$$

Equations (2.11) and (2.15) give us the following set of linear equations:

$$\begin{pmatrix} 1 & -\sin \vartheta_0 \\ 4h & -2c\delta \tau_{S0} \end{pmatrix} \cdot \begin{pmatrix} d \\ R_0 \end{pmatrix} = \begin{pmatrix} h \\ c^2 \delta \tau_{S0}^2 \end{pmatrix} \quad (2.16)$$

This equation may be solved by standard methods. One needs a TDOA between the two paths and an angle of arrival ϑ_0 to determine the depth of the source. In this regard, we may refer to part II.A.2.ii where a three-hydrophone array enables one with two TDOAs to find an azimuth γ and an elevation angle ϑ . If we situate ourselves in the plane given by the hydrophone H_0 , the source S and the projection of S onto the hydrophone plane array, the depicted situation in this part comes back to assimilating ϑ_0 to ϑ , that is to say $\vartheta_0 = \vartheta$. By applying this method to a three-hydrophone array and by determining the elevation angle ϑ , we may therefore obtain the depth of the source.

In this regard, part II.A.2.ii states that the arriving angle ϑ_0 , which is the elevation angle, is either positive or negative because the \cos function is pair. Therefore, the sign $\sin \vartheta_0$ depends on the angles sign. That means that there are two possible values of $\sin \vartheta_0$ and thus two different values of the depth d . As supposed in part II, we consider only positive values of ϑ by pretending that the deep diver cetaceans are located under the array. In this effect, with the resolution of equation of equation (2.16) one may express the depth d as such:

$$d = \frac{\sin \vartheta_0 c^2 \delta \tau_{S0}^2 - 2hc\delta \tau_{S0}}{4h \cdot \sin \vartheta_0 - 2c\delta \tau_{S0}} \quad (2.17)$$

2 - Numerical simulation

We simulated via a MATLAB script *depth_loc.m* the previous depth finding method. First of all, the elevation angle ϑ has to be found with the direction finding program depicted in part II.A.2.ii. Hence, the presented Matlab script results from the previous program. The azimuth is not an influencing parameter, that is why we may simulate the results by only changing the elevation angle.

For the simulation, we placed the source at a fixed distance r and bearing γ then changed the elevation angle from 0 to 180° , given that we consider only the elevation angles on one side of the plane array (here the positive angles for the simulation). Contrary to the previous localization method, the depth of the array matters here. In this regard, the adopted data for the simulation is given below:

- depth of the hydrophone array $h = 80m$,
- distance between the hydrophone H_0 and the source $r = 8000m$,
- azimuth of the source location $\gamma = 40^\circ$,
- sound speed $c = 1500 m \cdot s^{-1}$,
- distance between two hydrophones $L = 0.5m$,
- position of the hydrophones: $H_0 = [0,0,0]; H_1 = [0, L, 0]; H_2 = [L, 0, 0]$,
- angle between the two pairs of hydrophones: $w = 90^\circ$,

i - Simulation without elevation angle errors

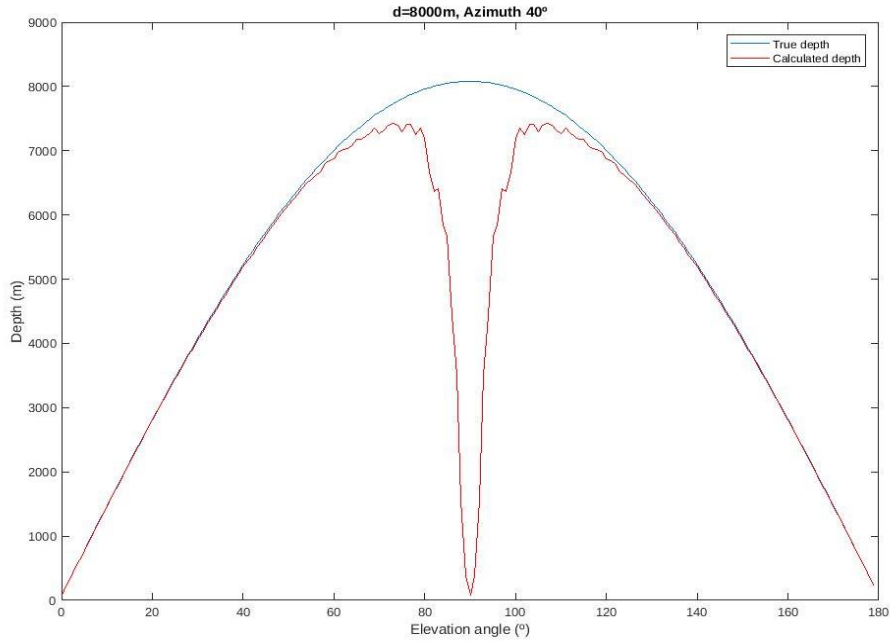


Figure 20 - Calculated and theoretical depth for a fixed distance and azimuth in function of the elevation angle

Figure 20 is a simulation of the depth localization method for a changing elevation angle ϑ . Similarly to the previous method, we simulated *via* the function *signal_received_by_one_hydrophone.m* the signal received by hydrophone H_0 to which we added the surface reflected signal. In this effect, we numerically simulated equation (2.17) with the time difference between surface-reflected and direct ray path measured with cross correlation. We may observe that the calculated depth drops drastically between 80° and 100° and that a minimum stands for $\vartheta = 90^\circ$, namely when the source is just underneath the array. This peak is coherent with equation (2.17) that states $d(90) = \lim_{\vartheta \rightarrow 90} d = h = 80m$. Thus, the peak is directly related to the expression of the equation. For an elevation angle of 90° , the results may then be distorted. For this matter, we will not consider the estimated depths measured for this elevation angle. This figure above was numerically simulated by implementing the measured TDOA between direct and surface-reflected paths and the correct values of the elevation angle ϑ .

However, we have noted previously that, even though the signals were filtered, the estimated angles contained errors. Be that as it may, for two different values of ϑ , the estimated depth will change. In this regard, elevation angle errors may give us incoherent depths (compared to the bottom depth for instance) or simply false values. A numerical simulation was carried out to show the estimated depth errors if the estimated elevation angles were not exactly correct. This simulation is stressed by figure 21 below.

ii - Simulation with elevation angle errors

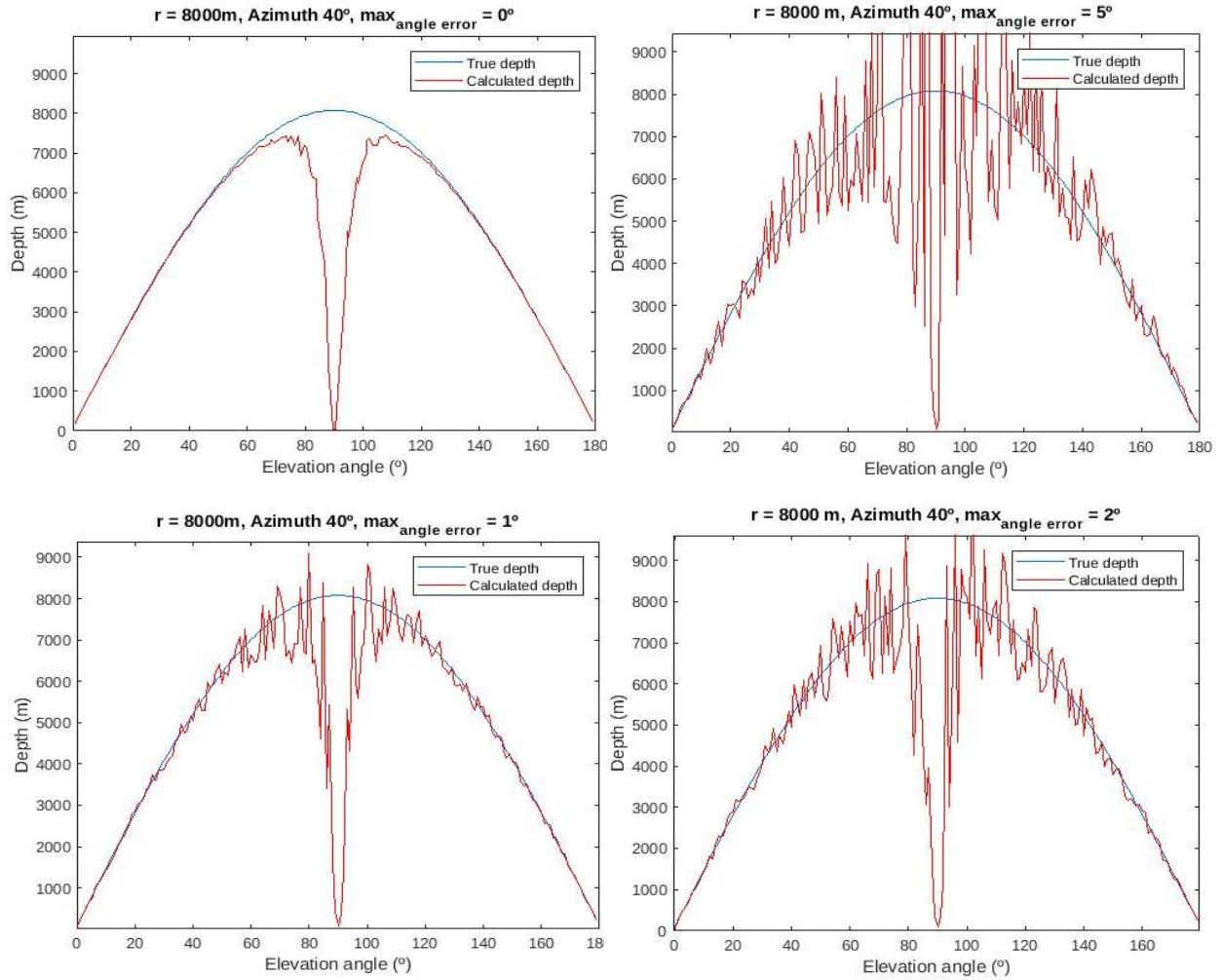


Figure 21 - Estimated depth depending on the estimated elevation error

For this particular numerical simulation, we carried out the same simulation as the previous figure 20 *i.e.* no angle errors (up-left panel). We simulated three other cases by implementing an error in the estimated angle. Indeed, equation (2.17) was calculated with the measured TDOA and we added a Gaussian error to ϑ_0 , respectively angle errors going up to 1° (up-right panel), 2° (bottom-left panel) and 5° (bottom-right panel).

It is notable that with greater angle errors, the estimated depth may differ completely from the true depth. For $\max_{\text{angle error}} = 5^\circ$, the estimated depth in the band $[40^\circ, 140^\circ]$ shows errors going from 300 m to more than 10 km (especially around $\vartheta = 90^\circ$). Likewise, for $\max_{\text{angle error}} = 2^\circ$ the estimated depth can differ by 2000 m around $\vartheta = 90^\circ$, whereas it may differ by 850 m for $\max_{\text{angle error}} = 1^\circ$. As explained earlier, the estimated depths for angles close to 90° may not be considered.

Nevertheless, the depth boundary is limited to the bottom depth. By referring to the seabed off Lisbon, figure 2 shows up depths of the area going up to 2500-3000m. The hypothesis of distant cetaceans (as numerically simulated above) should therefore estimate small or big elevation angles, that is to say that we may focus on the two ends of each graph. We may thus highlight the fact that the estimated depths correspond more to the true depths, even though the errors for $\max_{\text{angle error}} = 5^\circ$ are bigger (up to 200-

300m). Therefore, for distant cetacean signals, the estimated depth may be taken into account. The limit of this hypothesis is that, even though we detect the signal, we do not know the range of the sea mammal. Small or big estimated elevation angles may be clues to distant animal locations but they are not sufficient enough to validate this first assumption.

In this part, we have developed two simple localization methods: sound source bearing finding and depth estimation. The main hypothesis we used to carry out these methods and simulate them numerically were: distant cetacean source, constant celerity and absence of marine mammals above the array. We have stressed the necessity of filtering the data to detect the signal of interest and use cross correlation for time arrival of difference measurement. The estimated azimuth and elevation angles may show some errors that can interfere with depth estimation. Even though, the bearing and depth localization methods are not the most accurate methods, they give the user an interesting notion of where the cetaceans are. The last problem is to correct these angles with the position of the array. Indeed, the angles are measured from the plane array. One has to know the orientation and the pitch-roll-yaw of the array to correct the estimated direction before estimating the depth. We may now confront these theoretical methods to experimental data collected off Lisbon's coast.

III - Application of localization methods to an experimental four-hydrophone array

As developed in the two previous parts, we had been working on the square configuration of a four-hydrophone array spatially constrained by the structure of the wave glider. As a substitution experiment to the Azores' experiment, our tutor provided us with data from an experiment off Lisbon's coast conducted from the 5th to the 7th of May 2019 in the frame of the SUB-ECO project. In this sense, we have reconfigured our previous work to carry out the methods we had been working on. The new array is now a six-hydrophone array arranged in a tetrahedron geometry. Nevertheless, the notion of spatial constraint is still present because of the arrays' dimensions. In this regard, an adapted array will be studied for localization issues. Eventually, cetacean may be detected and localized.

A - The localization experiment

The new six-hydrophone-array experiment enables us to define a new geometry to which we will adapt the localization methods. Exploitation of the data and detection will therefore be studied.

1 - The experiment

The experiment consists in hanging an acoustic array under a buoy connected to a satellite. As shown on figure 22, the buoy contains a datalogger and is linked to the array via an umbilical cord through which transmits the recorded data. The experiment focuses mainly on the array and the collected data. That is why we will not develop the programming of the equipment used during this experiment given that it not the main point of the project.

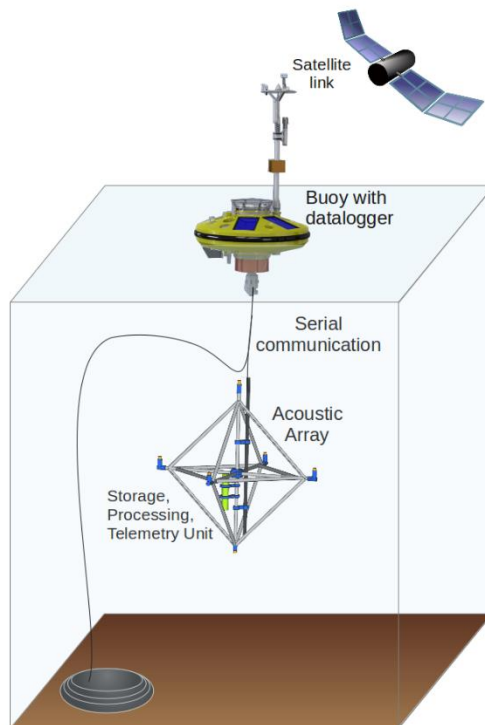


Figure 22 - Representation of the diamond hydrophone array (intern source)

The array is arranged in a tetrahedron where each hydrophone is placed at 0.75 m from the centre. The upper hydrophone is the first channel. Channels 2,3,4,5 in the centre square (clockwise) and channel 6 at the bottom. Hydrophone 2 is heading towards the magnetic north thanks to a magnetic compass. We have decided to proceed to localization with this experiment even though it does not correspond exactly to the expected experiment of the Azores.

In order to cohere with the previous simulation work we had made for the Azores' experiment, we decided to adapt the study of this new array and to exploit only the data of the square array *i.e.* hydrophones 2 to 5. The array is therefore a planar four hydrophone array where every hydrophone is spaced by 0.75 m from the array's center. The spatial constraint imposed by the wave glider is not exactly respected but the dimensions of the array seem small enough to consider this substitution data and apply it to the previous models. For the two localization methods, we therefore used the following data:

- sound speed $c = 1530 \text{ m} \cdot \text{s}^{-1}$,
- distance between two hydrophones $L = 1.0607 \text{ m}$,
- position of the hydrophones: $H_2 = [0, 0, 0]; H_3 = [0, L, 0]; H_4 = [L, L, 0]; H_5 = [L, 0, 0]$,

2 - The exploitation of the data

This experiment provided us with 240 thirty-second audio files (.wav) containing each 6 channels, one for each hydrophone. These hydrophones recorded data with a sampling frequency of 52734 Hz. As explained in part II.A, the frequency method detection was chosen for the processing of the data because it was more adapted considering the type of data and the area where it was collected.

i - Detection and filtering

The first thing to do is to filter all the audio files. Indeed, our first reflex was to listen to some files and there was no doubt about sea mammal presence thanks to audible cetacean whistles on many audio files. Yet, these signals were covered by noise (self-noise and ambient noise). These data were particularly noisy at low frequencies (between 0 and 5000 Hz). As one may see on the left panel spectrum of figure 23, it is hard to exploit frequency information from raw data, whereas the second spectrum (right panel) shows a peak frequency around 12 kHz, which may interest us for mammal detection.

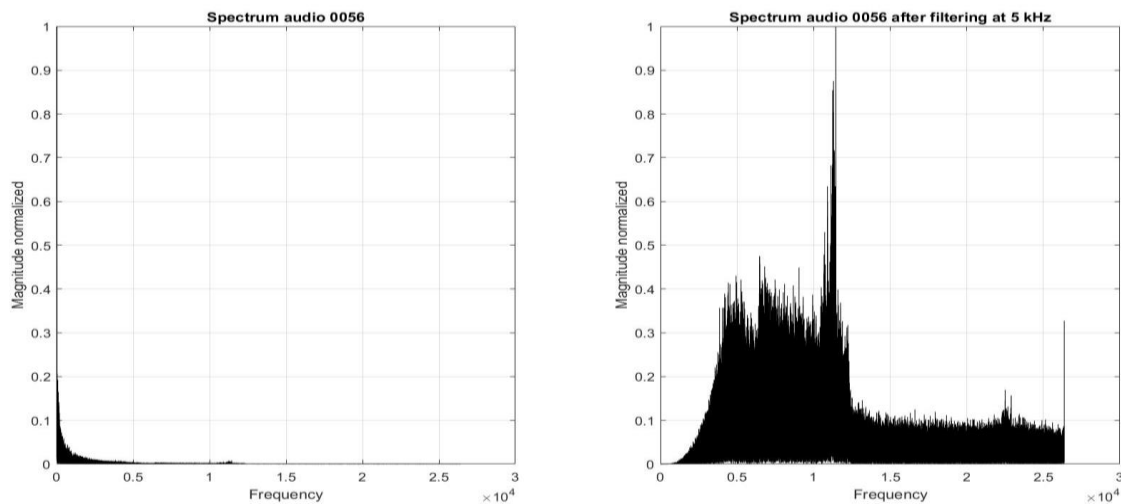


Figure 23 - Comparison of two spectrums of the audio file 0056 before (left panel) and after (right panel) filtering (intern source)

Thus, we applied a 5 kHz high-pass filter on all audio files and plotted their spectrum. This enabled us to select the audio according to their frequency content: we chose samples with frequencies of interest. We searched for two types of frequency information: frequency peaks around 12 kHz, audible on the recordings that seemed to correspond to dolphin whistles and high frequency concentration above 15 kHz, which sounded like clicks (figure 24).

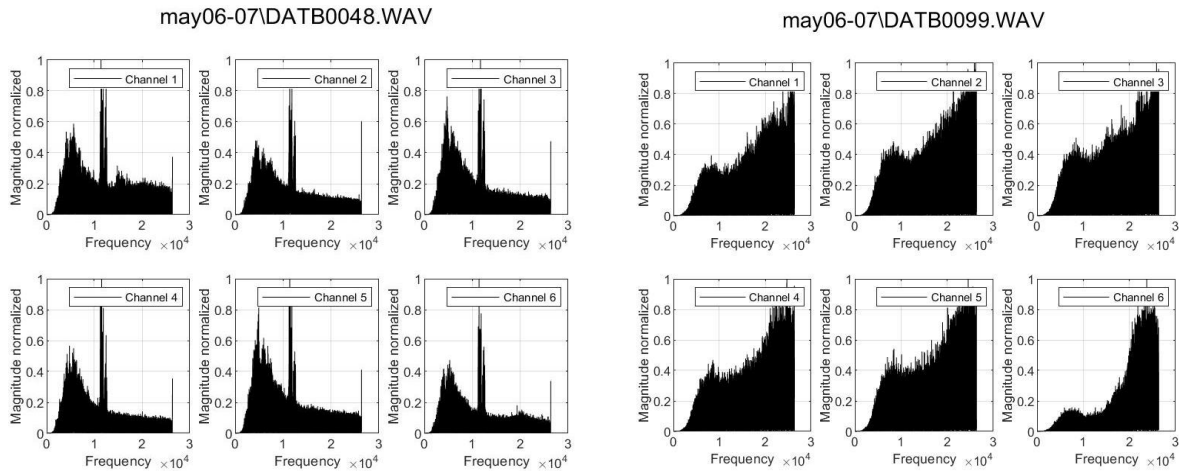


Figure 24 - Spectrums of files 0048 (left panel) containing frequency peak around 5 kHz and 12 kHz and 0099 (right panel) with a concentration of acoustic energy above 20 kHz (intern source)

In this way, we have found many audio files figuring cetacean sounds. To push the analysis further with a more accurate frequency analysis, the spectrograms of the selected samples were plotted. This method was only used at this stage of the treatment because the algorithm is very greedy in memory and the complexity makes it time consuming because of the high sampling frequency. Two different type of cetacean signals are shown on figure 25 and 26: communication signals such as whistles and echolocation clicks.

ii - Cetacean whistles

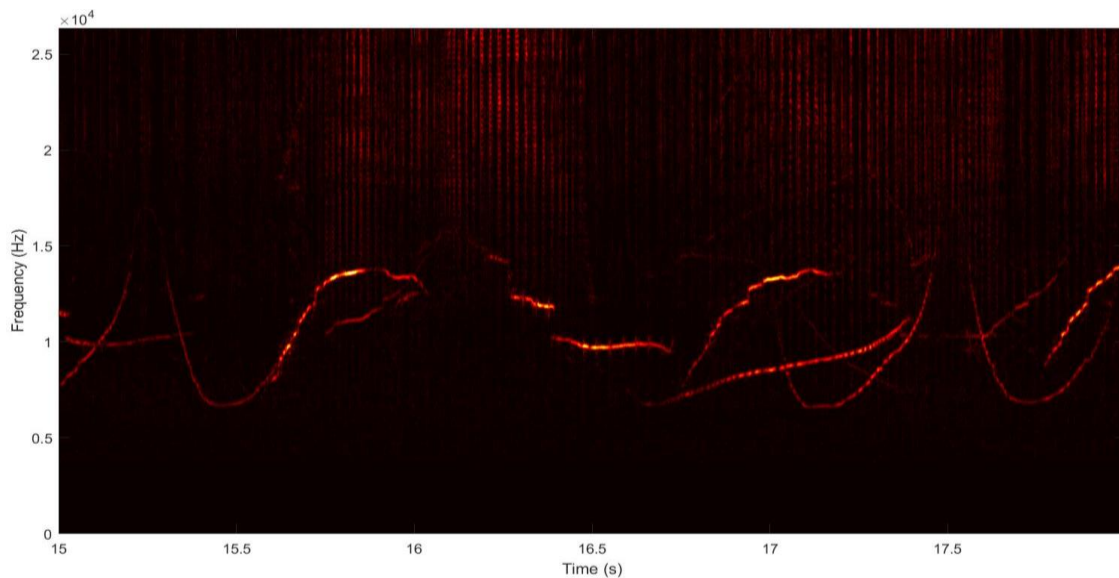


Figure 25 - Spectrogram of cetacean whistles (source: intern data 043.wav)

Figure 25 represents the spectrogram of the 043.wav audio file and the concentration of energy underscores whistles that we assume were dolphin whistles. In this effect, the peak frequencies correspond to dolphin whistle frequencies. Throughout this project, we chose not to study the classification of cetacean sounds, so we may not assert to which specie exactly these whistles correspond. Nevertheless, we contacted a former “oreille d’or”, M. Dréo *via* our teacher in charge of underwater acoustics class that confirmed hearing a common specie of dolphin. In this sense, we may make the assumption that the detected signal refers to dolphin signals. On the one hand, for low frequencies, the spectrogram appears to be very dark, that is to say that there is no energy. In fact, this absence of energy comes directly from the high-pass filter (>5 kHz). On the other hand, for frequencies over 10 kHz, some sort of rays that refer to echolocation clicks seem to come out but they are difficult to exploit. Conversely, figure 26 shows echolocation clicks without any whistles.

iii - Cetacean echolocation clicks

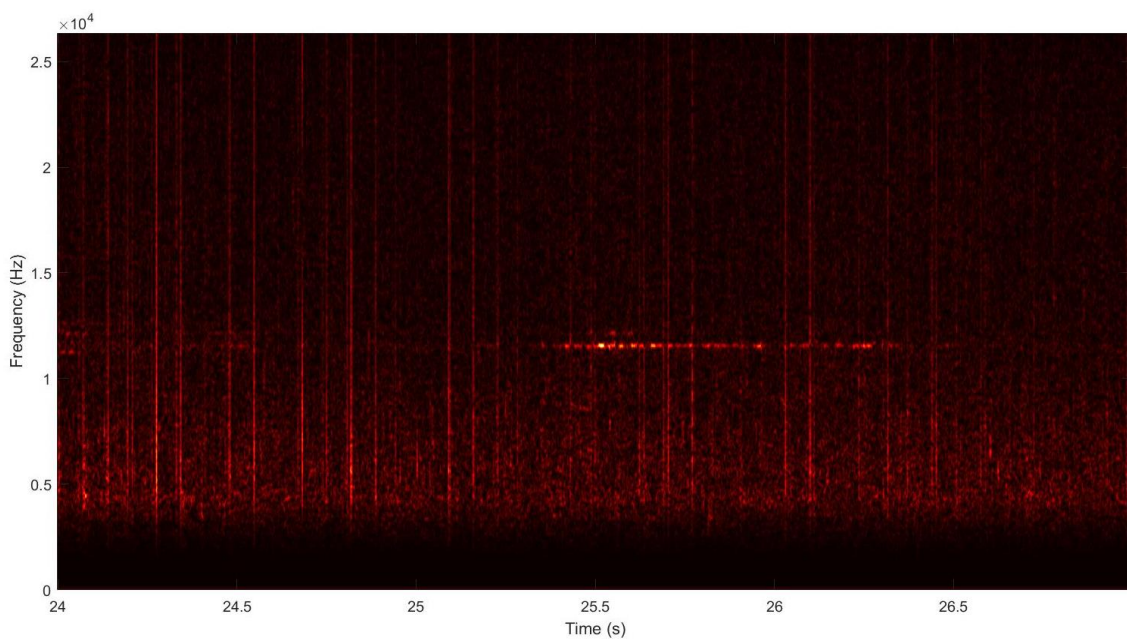


Figure 26 - Spectrogram of cetacean clicks (source: intern data 146.wav)

The other signals that were present in some samples were echolocation clicks. As developed in *I.A.2.ii*, these clicks are short time pulses of highly significant intensity that are more suitable for localization issues. Figure 26 pictures a sample where we were able to figure out some echolocation clicks. It is notable that the clicks show some frequencies going up to more than 25 kHz, inaudible frequencies for the human ear. As mentioned above, we did not focus on cetacean classification. However, these frequency characteristics and the measured ICI correspond to underwater mammal signals. We also assumed these clicks originated from dolphins, but we do not dispose of enough information and classification algorithms to confirm this hypothesis and to define the correct specie. Nevertheless, the feedback of M. Dréo confirmed the hypothesis of dolphin echolocation clicks. Like the previous figure, the filtered signal does not feature very low frequencies. Furthermore, one may observe a constant highly significant frequency of 12 kHz throughout the whole sample. These clicks are therefore the signal that we may consider for a localization purpose.

3 - Time Difference Of Arrival measurement

As highlighted in part II.A., TDOA measurement with cross-correlation is necessary. To achieve this, one should determine the most relevant and adequate type of signal for this type of processing. Signals must be easily detectable with the least amount of noise possible. Moreover, in order not to mix up the same part of the signal between two channels, we wanted to calculate a TDOA with a sound variation which must be isolated and brief enough in the time domain. Indeed, the confusion of two sound pressure variation between two hydrophones could distort the TDOA results. As simulated in part II, we expect the TDOA values to have 10^{-4} s magnitudes. For localization issues, we will study TDOA measurement for the two types of signals: communication signals and echolocation clicks.

i - Whistle TDOAs

Whistles are vocalisations particularly powerful in energy with a normalized sound level up to -10 dB on experiment recordings as one can see on figure 27. That is why they are easy to detect. Here, communications are enhanced on the graph over the time scale [5,9]s. Moreover, this energy is concentrated around an audible frequency of 12 kHz which is a frequency in the middle of record band of our sensors. This phenomenon expresses itself by a sound pressure variations over tenths of seconds which may be too long to be accurate enough compared to the expected values of TDOAs.

Often these whistles do not appear isolated as it is shown on the spectrogram of audio 057.wav. As brought out by figure 28, the time domain signal which corresponds to the sample used to draw the previous spectrogram does not show isolated variations of the signal that we may easily find on each channel. In this regard, cross-correlation is difficult to process. We may note that the two plotted figures show also echolocation clicks.

Consequently, even though we may easily detect these whistles, they are too complicated to study in the time domain in regard of cetacean localization issues. Time difference of arrival measurements are difficult to distinguish given that we do not always know exactly which signal corresponds to which whistle.

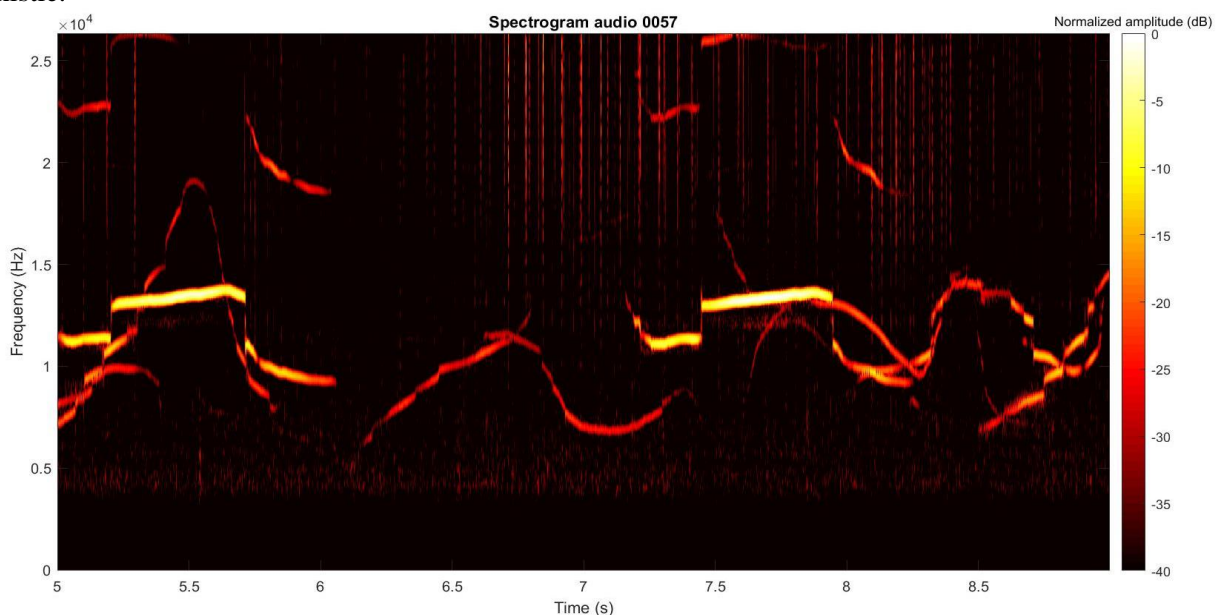


Figure 27 - Spectrogram of cetacean whistles and clicks (source: intern data 057.wav)

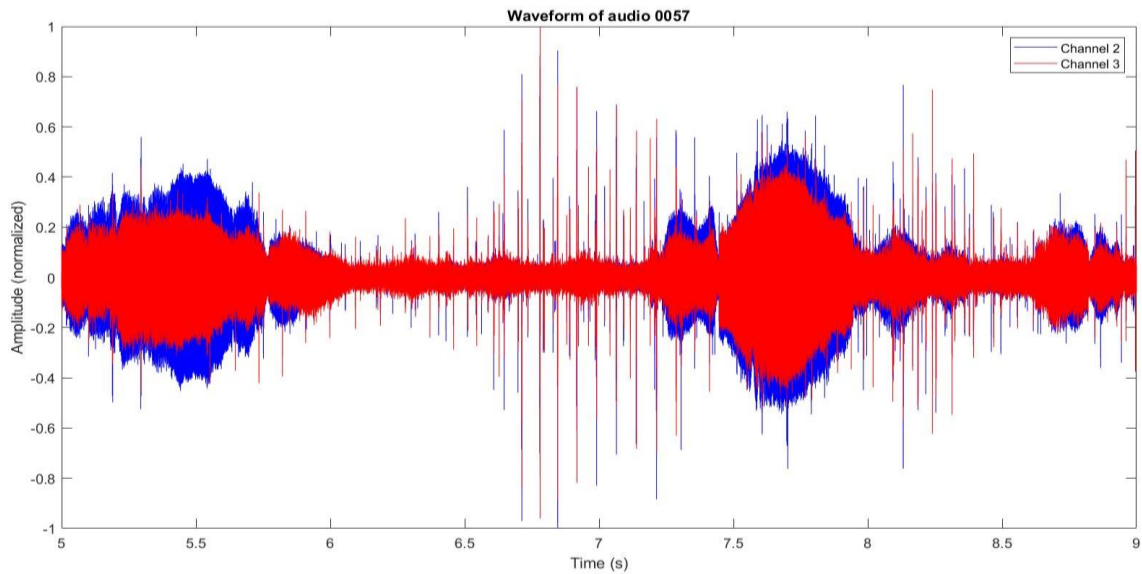


Figure 28 - Waveform of cetacean whistles and clicks (source: intern data 057.wav)

ii - Echolocation click TDOAs

The second type of signal of interest is echolocation clicks. These vocalizations do not seem at first glance the easiest ones to detect because they are often hidden by ambient noise. However, after processing and filtering a sample, echolocation clicks are much more easily detectable and seem to have all the characteristics we are looking for. Indeed, as shown by figure 29 and 30, respectively in the frequency and time domain, it appears that after filtering these clicks were easily detectable and particularly identifiable. Furthermore, the short duration of their variation, about a thousandth of a second, enables one to simply isolate them temporarily. Thus, TDOAs may be calculated between the same clicks on different hydrophones. Echolocation clicks are therefore more suitable for localisation issues.

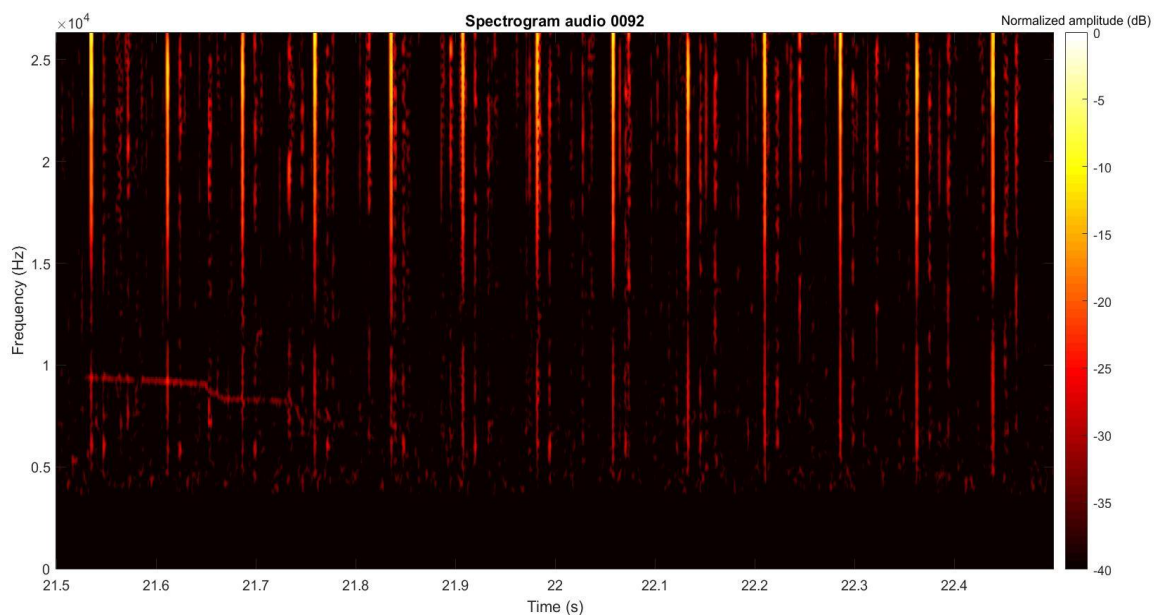


Figure 29 - Spectrogram of cetacean clicks, audio 092.wav (source: intern data 092.wav)

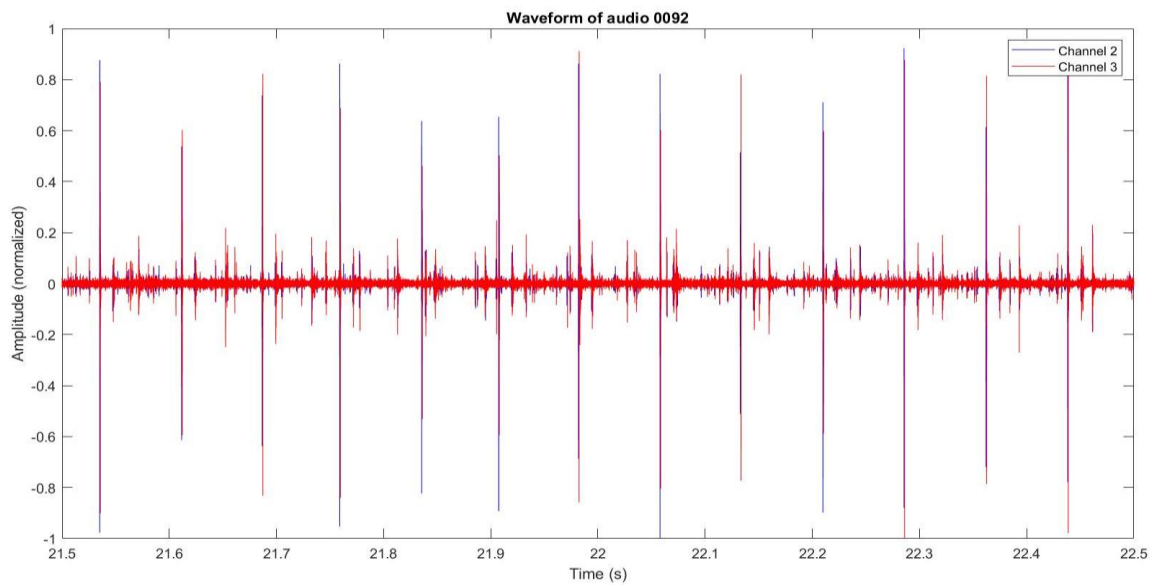


Figure 30 - Waveform of cetacean clicks, audio file 092.wav (source: intern data 092.wav)

Furthermore, we may isolate a single click on two different channels and distinguish several interesting information (figure 31). The first click (at $t = 22.0575$ s for channel 2 and $t = 22.0582$ s for channel 3) has a much greater amplitude than the following clicks. It is also notable on the spectrogram of figure 32 that the energy of the click is much higher than the next clicks. This click is more likely to be signal stemming from the direct acoustic ray path between the cetacean and the hydrophone array. As explained in part II-B, our bearing localization algorithm is based in direct ray path signals. Given the depth of the hydrophone array (80 m), it seems that the first attenuated click may correspond to the surface reflected ray path ($t = 22.06495$ s for channel 2). The next attenuated click seems also to be an attenuated click that may correspond to the bottom-reflected signal. All these clicks from the same signal recorded on several hydrophones enable the measurement of TDOAs and the application of different localization methods.

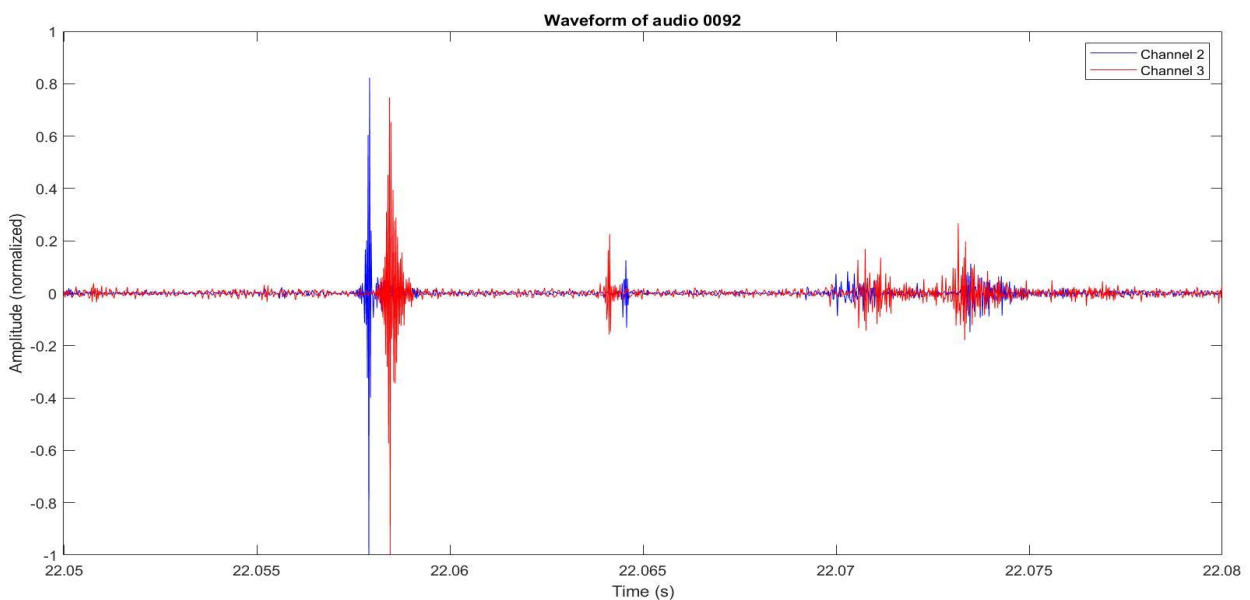


Figure 31 - Waveform of isolated cetacean clicks on channels 1 and 2 (source: intern data 092.wav)

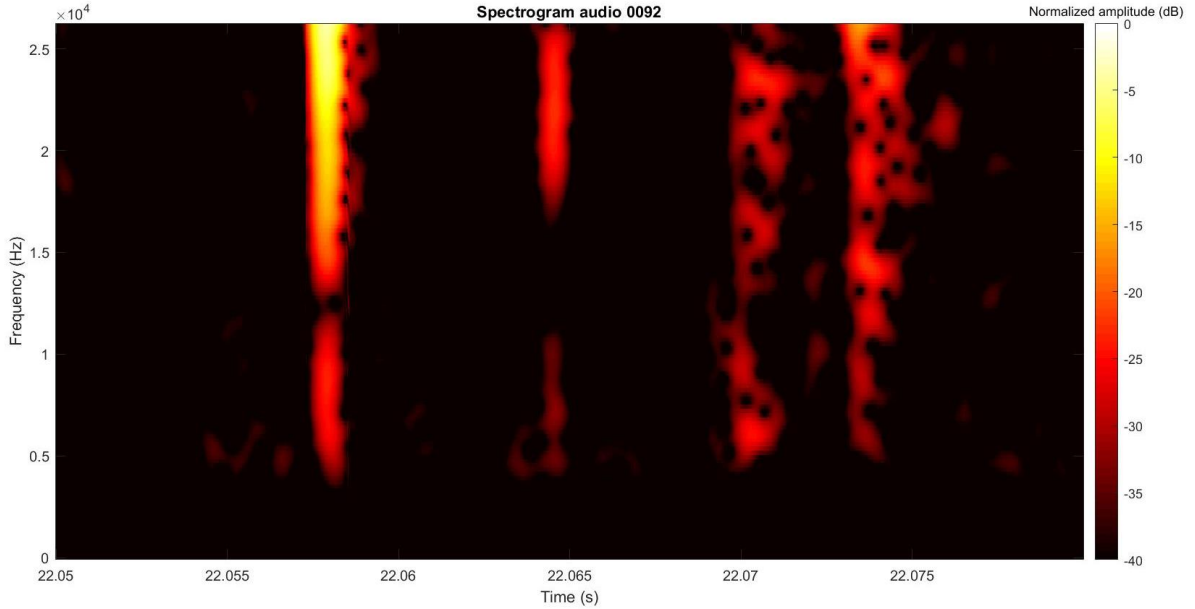


Figure 32 - Spectrogram of isolated cetacean clicks of channel 2 (source: intern data 092.wav)

B - Results and analysis

We have highlighted previously the presence of cetacean signals in certain samples. We will now estimate the bearings and depths of the sources of the received signals. Even though we cope with echolocation clicks and we are not trying to classify the specie, some information tend to suggest the presence of dolphins. Dolphins are not deep divers and the array is hung at an 80 m depth. Therefore, it is probable that some cetaceans may be present above and under the array. The hypothesis of only positive elevation angles is thus not valid anymore. For the following results, we will only be showing the absolute values of this angle. Nevertheless, one must keep in mind that there are two possible values.

1 - Bearing estimation

i - Bearing results

After filtering the audio files, choosing the data of interest and measuring several TDOAs, we may now proceed to bearing estimation. As a reminder, the square array is composed of hydrophones 2 to 5 (clockwise) with hydrophone 2 facing the magnetic north. For the numerical simulation, we programmed the array as such: $H_2 = [0,0,0]$; $H_3 = [0, L, 0]$; $H_4 = [L, L, 0]$; $H_5 = [L, 0, 0]$. The magnetic azimuth is easily obtained by adding the heading correction to the calculated azimuth angle (example in appendix B). Nevertheless, we will not focus on the exact true bearing but only on the angles directly estimated with the MATLAB program *bearing_loc.m*. To correlate the estimated angles, we will carry out the direction-finding method of part II.B (that only applies to a three-hydrophone array) to two sets of three-hydrophones: $[H_2, H_5, H_3]$ and $[H_2, H_5, H_4]$.

A first estimation was made with the audio file 0094.wav which happened to show cetacean clicks, for an eleven click series in the time band $[5.51, 6.15]$ s. In order to use the two sets of three-hydrophones, we measured three TDOAs (for the pairs H_2H_3 , H_2H_4 and H_2H_5) between two clicks that are all sorted chronologically into Table 1 (columns 1 to 3). Using these TDOAs we estimated with the

bearing_loc.m program the azimuth and elevation angles for the two sets $[H_2, H_5, H_3]$ and $[H_2, H_5, H_4]$. In order to clarify Table 1, only two digits after the decimal point are shown even though the estimated TDOAs and angles showed up to fifteen decimal places.

TDOA1 (s) H2 H3	TDOA2 (s) (H2 H4)	TDOA3 (s) (H2 H5)	Azimuth (°) using H2 H5 H4	Azimuth (°) using H2 H5 H3	Elevation (°) using H2 H5 H4	Elevation (°) using H2 H5 H3
-2,84E-04	-9,27E-04	-6,81E-04	19,86	22,62	180 - 17.13i	180 - 20.52i
-4,92E-04	-8,33E-04	-3,22E-04	57,80	56,82	150,59	148,01
-4,91E-04	-8,32E-04	-3,21E-04	57,80	56,82	150,46	147,89
-4,91E-04	-8,31E-04	-3,21E-04	57,80	56,82	150,40	147,84
-2,27E-04	-8,70E-04	-6,81E-04	15,52	18,43	180 - 11.10i	180 - 15.06i
-4,91E-04	-8,32E-04	-3,21E-04	57,80	56,82	150,46	147,89
-2,27E-04	-8,69E-04	-6,80E-04	15,52	18,43	180 - 10.90i	180 - 14.92i
-4,91E-04	-8,31E-04	-3,21E-04	57,80	56,82	150,40	147,84
-4,91E-04	-8,12E-04	-3,21E-04	56,82	56,82	147,84	147,84
-2,46E-04	-8,88E-04	-6,62E-04	18,92	20,38	180 - 7.65i	180 - 10.88i

Table 1 - Azimuth and Elevation angles calculated the audio file 0094.wav between 5.51 and 6.15s

The first thing we may note is that the values of the TDOAs correspond to the expected magnitudes. We may also observe real and complex angles. Of course, complex angles do not describe the reality of the situation. By looking closer at the results of the complex angles, the equation (2.3) gave us $|\cos\beta_i| = \left| c \cdot \frac{\delta\tau_{i0}}{L_i} \right| > 1$. These complex numbers may therefore have different origins regarding the hypothesis of constant celerity and distant sound source, that is why $|\cos\beta|$ may be superior to 1. By looking at the corresponding TDOAs, we may note that they have similar magnitudes. Hence, one may suggest that they are emitted by the same source even though we are not able to localize it.

Nevertheless, the six other results depict similar magnitudes for the TDOAs and the calculated angles. In the same way, we may assume that these clicks come from at least the same location. One may notice that the estimated azimuth angles are approximately the same with different clicks for each set of hydrophones and that the difference between the two hydrophone sets equals to 1° . Likewise, the elevation angles show angle differences up to 2.5° .

ii - Analysis

We modeled onto a graph (figure 33) these estimated angles for three different files that happened to possess cetacean clicks. For a pair of click, we estimated two locations: one for each hydrophone sets. For each audio file, we considered ten clicks. Is represented on the graph only the angles that were real. We assumed that the complex angles did not suit enough the hypothesis made for this project. We distinguished the angles measured with each set of hydrophones with crosses ($[H_2, H_5, H_3]$) and circles ($[H_2, H_5, H_4]$). Likewise, each audio file location estimation is portrayed with a colour code (blue for 131.wav, black for 239.wav and red for 094.wav).

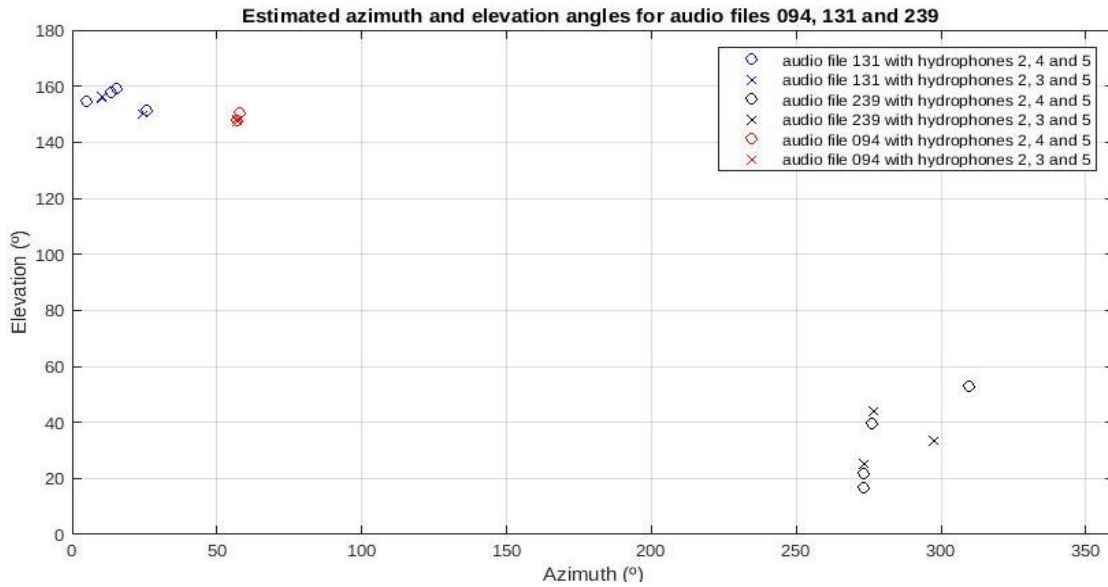


Figure 33 - Estimation azimuth γ and elevation angle ϑ with clicks from three different audio files

This graph enhances the different angles estimated with different audio files. It appears obvious that for some audio files such as 094.wav, the estimated locations of the sound source for different clicks are grouped, whereas they are scattered for other files (for instance 239.wav). By looking closer to files such as 239.wav, it is noteworthy that the measured TDOAs differ which explains the unequal distribution of each location points of the file. However, even in a same file, location points are grouped. Considering that we are studying clicks in a one second sample, even though the waveform of the signal seems to picture the same clicks, it is possible that the hydrophones collected information from different cetaceans. As a matter of fact, the array may have localized more than one cetacean. In this sense, grouped location point suggest the presence of at least one cetacean (given that cetaceans may travel in group, they would be spotted at the same location). When the clicks are not grouped, we may suggest two different assumptions: either the hypothesis made lead up to too big location errors, either there are several cetaceans that emit echolocation clicks. In regard of the second assumption, the audio file 094.wav would present at least one cetacean whereas 131.wav would show at least two cetaceans. Lastly, we assert that a slight difference of angles between the true and calculated bearing will lead to big errors for distant sources.

2 - Depth estimation

i - Depth results

We estimated the depth of the source present in the audio file 094.wav. First of all, we corrected the measured elevation angle with the actual pitch/roll angles at the time of study. In this regard, we had tables of the correction angles for each sample throughout time. Appendix B shows for a short amount of time the pitch-roll-yaw angles. The moment of interest for which we had made measurements in the previous part is highlighted and gave us a pitch angle of 21.83° and a roll angle of -10.54° . As mentioned earlier, we will not focus on the exact heading of the array. The angle of interest for this correction is the pitch angle. Thereby, we have corrected the estimated angles with this given pitch angle. For the corresponding angles of Table 1, we selected what we thought to be the reflected path ray signals and measured TDOAs onto hydrophone 2.

Afterwards, TDOAs had to be measured on the same hydrophone. We chose to study channel 2 exclusively. Considering a depth of 80m for the array, the expected TDOAs between the two ray paths, namely direct and surface-reflected paths, should not theoretically exceed $(2*80)/1530 = 0.105$ s. This part was the most difficult one. It is very very hard to distinguish on the same channel the direct path signals and the surface-reflected ones that correspond to the same click. Indeed, an attenuated signal may not always be the surface reflected signal. It is thereby complicated to associate the direct path and surface-reflected path signals.

TDOA (s) H2	Elevation (°) ϑ 254	Elevation (°) ϑ 253	Depth (m) 254	Depth (m) 253
0.0391	157.87	156.21	159.92	189.01
0.041	154.72	156.25	205.4	174.6
0.047	157.81	156.15	132.09	147.04
0.064	154.73	156.25	115.56	109.82
0.069	157.92	156.25	99.69	103.93
0.075	158.98	156.25	93.2	98.17

Table 2 - Calculated depths of file 131.wav for the positive values of the elevation angle

TDOA (s) H2	Elevation (°) ϑ 254	Elevation (°) ϑ 253	Depth (m) 254	Depth (m) 253
0.0391	-157.87	-156.21	39.34	39.62
0.041	-154.72	-156.25	39.45	40.08
0.047	-157.81	-156.15	45.14	44.45
0.064	-154.73	-156.25	55.54	56.02
0.069	-157.92	-156.25	59.67	59.19
0.075	-158.98	-156.25	63.6	62.91

Table 3 - Calculated depths of file 131.wav for the negative values of the elevation angle

Tables 2 and 3 were simulated with the angles that the program *bearing_loc.m* calculated in part II.B.1 (cf Table 1). Likewise, two depths were measured with one angle, one for each set of three-hydrophones. As mentioned previously, dolphins do not dive deep and may therefore be between the array and the surface. That is why figures on the tables for one TDOA, the two different values of the elevation angle were simulated.

ii - Analysis

We may first note that the calculated depths do not seem absurd given that if ϑ is positive *i.e.* the source is under the array, we find depths over 80m, whereas if ϑ is negative, we find a source depth between the array and the surface.

As stated above, finding a click and its surface-reflected signal is hard. In this sense, we have exploited 131.wav. Nevertheless, other files we had used for the bearing-finding method because they presented easily identifiable clicks were not exploitable at all. The SNR was sometimes too low to distinguish clearly the attenuated peaks of the signal. Among the selected files for the first method of selection, only a few of them were usable. In this regard, this second method is much less liable than the first one.

When it comes to the results, for a sample of one second on an audio with six studied TDOAs, we obtain varying depths. At first glimpse, the measured depths point out similar results: going from 93.2m to 189.01m in the case of positive elevation angles, and from 39.34m to 62.91m in the case of negative elevation angles. Even though there is up to a 100m difference, we may note that the magnitude of the depth seems to refer to a close depth location. First, these results show that for different elevation angles, the estimated depth can significantly change. However, as mentioned with the analysis of the first method. These locations may refer to different cetaceans. In this case, considering the received signal, the clicks seem to have the same characteristics and to come from the same source. Nevertheless, we may assume that there is only one cetacean but we do not have enough information to confirm this, especially regarding classification. However, given the estimated depth and angles, we may note that the source is not so distant. The hypothesis of distant source is here questioned by the obtained results.

This method is much wobblier compared to the previous one. Indeed, a first uncertainty intervenes when we use the first method to measure an angle used in the program *depth_loc.m*. Afterwards, another uncertainty is linked to the signal itself. As a matter of fact, it is very difficult to distinguish the amplitude variations and associate a click with its surface-reflected signal. On a sample, many attenuated signals are recorded and one may not always know if it was emitted by the same sound source.

Conclusion

Localizing using PAM methods, whether it is cetaceans or submarines, is a tough topic of actual study. For this Final Year Project, we focused on the localization of cetaceans with a four-hydrophone array constrained by the dimensions of a wave glider AUV.

We first studied characteristics of these mammals' signals and the environment in which they evolved. Subsequently, various simulations were conducted in order to understand this underwater acoustic phenomenon. It enables us to base the rest of the study on several hypothesis whose relevance were discussed and evaluated.

As a first intention to dimension a four-hydrophone array fixed to a wave glider, we focused on the characteristic of a close spaced hydrophone array. Taking in account these space constraints, we then studied two different models of localization. In this matter, we exposed a bearing-finding method and a depth estimation one that we numerically simulated and discussed.

Thereafter, we obtained from our tutor data from an experiment conducted in May off Lisbon's coast. As a matter, this data was a substitution to the experiment of the Azores that had been postponed during our stay in SIPLAB. We adapted the use of the six-hydrophone array in tetrahedron geometry into a four-hydrophone square, in accordance with our previous work on the JONAS experiment. We continued to lead the study of localization in this new environment. We processed the data to obtain signals of interest, namely cetacean signals, that we exploited in order to process our localization algorithm and methods.

This final phase gave us interesting results for localization issues. Echolocation clicks were detected, filtered and TDOAs were measured in order to obtain bearing and depth estimations. The convergence of some information made us assume that dolphin signals were present on the audio samples. In some audio files, clicks referred to a same location. In this regard, this location referred to at least one cetacean, but also to a group of cetaceans travelling together. On other files, different clicks referred to different locations meaning that either there were different cetacean signals or that some hypothesis made at the beginning of the study were too wobbly. Obviously, these results gave us an idea of where the sound source was, but the accuracy of the methods were discussed. We may as an extent to this project consider a celerity variation and the actual ray paths taken by sound given that they are not straight lines.

Appendix A - Matlab functions

```

function [T1,T2,T3,signal_1,signal_2,signal_3]=signal_received_by_array(c,L,H1,H2,H3,source,signal,t)
% c celerity (constant)
% L distance between each hydrophone
% H1 to H3 positions of hydrophones 1 to 3
% source position of the sound source
% signal emitted by the source, signal_i signal received by one hydrophone
% T1 to T3 time of arrival, t time of "listening"
% hydrophone 1
T1=sqrt((H1(1)-source(1))^2+(H1(2)-source(2))^2+(H1(3)-source(3))^2)/c;
[ind.row1,ind.ind1]=find(t>T1);
signal_1=circshift(signal,[0,ind.ind1(1)])+rand(1,length(t)); % time delay and noise adding
% hydrophone 2
T2=sqrt((H2(1)-source(1))^2+(H2(2)-source(2))^2+(H2(3)-source(3))^2)/c;
[ind.row2,ind.ind2]=find(t>T2);
signal_2=circshift(signal,[0,ind.ind2(1)])+rand(1,length(t)); % time delay and noise adding
% hydrophone 3
T3=sqrt((H3(1)-source(1))^2+(H3(2)-source(2))^2+(H3(3)-source(3))^2)/c;
[ind.row3,ind.ind3]=find(t>T3);
signal_3=circshift(signal,[0,ind.ind3(1)])+rand(1,length(t)); % time delay and noise adding

function [acor,tempscor,TDOA]=crosscorr_TDOA(t,signal_1,signal_2)
% t time scale
% signal1, signal2 the two signals to cross correlate
N=length(t);
pas=max(t)/N; % needed for timeDiff cf after
%cross correlation between sig1 and sig2
[acor,lag] = xcorr(signal_2,signal_1);
[~,I] = max(abs(acor));
acor=acor./max(abs(acor));
TDOA = abs(lag(I)*pas); % convert indices in time for the scale of schemas
tempscor=lag.*pas; % convert TDOA in time for the respective scale

function [TDOA_t1,TDOA_t2,TDOA_cc1,TDOA_cc2]=compare_TDOA(c,L,H1,H2,H3,d,Az,Elev,signal,t)
% c celerity (constant)
% L distance between each hydrophone
% H1 to H3 positions of hydrophones 1 to 3, (d,Az,Elev) spherical source position of the sound source
% signal emitted by the source
% t time of "listening"
% d distance, Az azimuth, Elev elevation of source (bearing)
% TDOA_t TDOA theoretic
% TDOA_cc TDOA calculates with cross-correlation
[x,y,z]=source_loc(d,Az,Elev); % source localization in cartesian coordinates from spherical coordinates
source=[x,y,z+80]; % hydrophone depth correction
[T1,T2,T3,signal_1,signal_2,signal_3]=signal_received_by_array(c,L,H1,H2,H3,source,signal,t);
[a1,b1,TDOA_cc1]=crosscorr_TDOA(t,signal_1,signal_2);
[a2,b2,TDOA_cc2]=crosscorr_TDOA(t,signal_1,signal_3);
TDOA_t1=abs(T2-T1);
TDOA_t2=abs(T3-T1);

function [Az_c, Elev_c]=bearing_loc(c,w,L1,L2,TDOA1,TDOA2)
% c celerity
% L1,L2 distance between hydrophones
% TDOA1,TDOA2 TDOAs of each hydrophone pair
% w angle between d1 and d2 (the two pairs of hydrophones)
%calculus of cosB1 and cos B2
cosB1=c*TDOA1/L1
cosB2=c*TDOA2/L2
% Azimuth Az and elevation Elev
Az_c=atand((cosB2-cosB1*cosd(w))/(cosB1*sind(w)))
Elev_c=acosd(cosB1/cosd(Az_c))

```

```

function [T,signal_1,R0,Rs]=signal_received_by_one_hydrophone(d,r,h,c,signal,t)
% c celerity (constant)
% signal emitted by the source
% t time of "listening"
% d depth of the source
% r range of the source
% h depth of the hydrophone
R0=sqrt(r^2+(h-d)^2); % length of direct acoustic path
Rs=sqrt(r^2+(h+d)^2); % length of surface-reflected acoustic path
T=(Rs-R0)/c; % true TDOA
[ind.row1,ind.ind1]=find(t>T);
signal_1=signal+circshift(signal,[0,ind.ind1(1)])+rand(1,length(t)); % time delay+signal adding+noise adding

function d=depth_loc(c,Elev,TDOA,h)
% c celerity
% TDOA time difference of arrival
% Elev elevation angle
% h depth hydrophone
% d estimated depth
d=((sind(Elev)*c^2*TDOA^2)-(2*h*c*TDOA))/((4*h*sind(Elev))-(2*c*TDOA))

```

Appendix B - Table results

TDOA1 (s) H2 H3	TDOA2 (s) (H2 H4)	TDOA3 (s) (H2 H5)	Azimuth (°) using H2 H5 H4	Azimuth (°) using H2 H5 H3	Elevation (°) using H2 H5 H4	Elevation (°) using H2 H5 H3
-2,46E-04	-8,14E-04	-5,49E-04	25,77	24,15	151,55	150,19
-2,46E-04	-8,14E-04	-5,49E-04	25,77	24,15	151,55	150,19
-1,13E-04	-7,75E-04	-6,24E-04	13,63	10,30	157,87	156,21
-1,14E-04	-6,81E-04	-6,24E-04	5,19	10,30	154,72	156,25
-1,13E-04	-7,75E-04	-6,24E-04	13,63	10,30	157,81	156,15
-1,14E-04	-6,81E-04	-6,24E-04	5,19	10,30	154,73	156,25
-1,14E-04	-7,76E-04	-6,24E-04	13,63	10,30	157,92	156,25
-1,14E-04	-7,76E-04	-6,25E-04	13,63	10,30	157,98	156,31

Table A - Azimuth and Elevation angles calculated the file 131.wav between 16.01 and 16.87s

TDOA1 (s) H2 H3	TDOA2 (s) (H2 H4)	TDOA3 (s) (H2 H5)	Azimuth (°) using H2 H5 H4	Azimuth (°) using H2 H5 H3	Elevation (°) using H2 H5 H4	Elevation (°) using H2 H5 H3
-6,25E-04	-6,25E-04	3,79E-05	-8,67E+01	-8,65E+01	16,83	25,49
-5,11E-04	-5,68E-05	2,65E-04	-5,05E+01	-6,26E+01	53,04	33,86
-6,25E-04	-6,25E-04	3,79E-05	-8,67E+01	-8,65E+01	16,83	25,49
-4,92E-04	-4,73E-04	5,68E-05	-8,39E+01	-8,34E+01	39,75	44,39
-6,25E-04	-6,25E-04	3,79E-05	-8,67E+01	-8,65E+01	16,83	25,49
-9,84E-04	-1,02E-03	-2,65E-04	7,07E+01	7,49E+01	180 - 31.71i	180 - 53.59i
-6,25E-04	-6,06E-04	3,79E-05	-8,66E+01	-8,65E+01	21,58	25,49
-6,44E-04	-4,92E-04	-2,46E-04	4,50E+01	6,91E+01	120,13	173,63

Table B - Azimuth and Elevation angles calculated the file 239.wav between 23.77 and 24.11s

Epoch timestamp (s)	roll (°)	pitch (°)	heading (°)
1494108227	21,43	-8,94	185,19
1494108230	20,91	-8,19	177,62
1494108233	21,83	-10,54	185,71
1494108236	20,28	-9,45	42,57
1494108239	21,77	-9,85	275,72
1494108242	20,57	-7,39	180,78
1494108245	21,08	-0,06	0,06
1494108248	21,43	-7,85	98,26
1494108251	20,45	-0,06	159,88

Table C - Correction angles for a 24s sample of 094.wav

Bibliography

- [1] Bagetoss, Paul M. 2013. *Processing advances for localization of beaked whales using time difference of arrival*. s.l. : Naval Undersea Warfare Center, 2013.
- [2] Dassati, A. *On-board Underwater Glider Real-time Acoustic Environment Sensing*. s.l. : NATO Undersea Research Centre, Laboratori d'Aplicacions Bioacústiques Universitat Politècnica de Catalunya.
- [3] Gassmann, Martin. *Offshore killer whale tracking using multiple hydrophone arrays*. 2013 : Scripps Institution of Oceanography.
- [4] Guillon, Laurent. 2019. *Acoustique Sous-marine UE8 EC2*.
- [5] Helble, Tyler A. 2013. *Site specific probability of passive acoustic detection of humpback whale calls from single fixed hydrophones*. s.l. : Scripps Institution of Oceanography, University of California, San Diego, 2013.
- [6] Hugues, David T. *Passive Acoustic Monitoring during the SIRENA 10 Cetacean Survey*. s.l. : NATO Undersea Research Centre.
- [7] Krim, Hamid. 1996. *Two decades of Array processing Research*. s.l. : IEEE SIGNAL PROCESSING MAGAZINE, 1996.
- [8] *Marine Acquisition Using Wave Gliders: A Field Feasibility Test*. Moldoveanu, Nick. 2014. s.l. : ResearchGate, 2014.
- [9] Tran, Duong D. 2014. *Using a coherent hydrophone array for observing sperm whale range, classification, and shallow-water dive profiles*. 2014.
- [10] Varma, Krishnaraj. 2002. *Time-Delay-Estimate Based Direction-of-Arrival Estimation for Speech in Reverberant Environments*. s.l. : Faculty of The Bradley Department of Electrical and Computer Engineering Virginia Polytechnic Institute and State University, 2002.
- [11] Wiggins, Sean M. 2010. *Monitoring Marine Mammal Acoustics Using Wave Glider*. s.l. : Scripps Institution of Oceanography, 2010.
- [12] —. 2013. *Tracking dolphin whistles using an autonomous acoustic*. 2013.
- [13] Zimmer, Walter M. X. 2005. *Echolocation clicks of free-ranging Cuvier's beaked whales*. s.l. : NATO Undersea Research Centre, 2005.
- [14] —. 2011. *Passive Acoustic Monitoring of Cetaceans*. s.l. : Cambridge University Press, 2011.
- [15] —. 2013. *Range estimation of cetaceans with compact volumetric arrays*. s.l. : Centre for Maritime Research and Experimentation, 2013.